FACULTY OF
COMPUTER SCIENCE

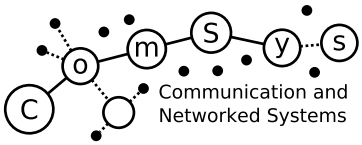

Communication and Networked Systems

Master Thesis

Swarm Communication in Space

Evaluating Ad-Hoc Routing Protocols for In-Situ Space Exploration Networks

Fin Christensen

Supervisor: Prof. Dr. rer. nat. Mesut Güneş
Assisting Supervisor: Dr.-Ing. Emanuel Staudinger (DLR),
MSc. Kai Kientopf

Institute for Intelligent Cooperating Systems, Otto von Guericke University Magdeburg

April 5, 2021

Abstract

Upcoming space exploration missions targeted on visiting extraterrestrial worlds like the surface of other planets and moons in our solar system demand new technologies due to more complex mission designs. The utilization of multiple robotic units during such missions enables the investigation of a broad surface area. By establishing communication channels between all the robotic units, a swarm of agents is created capable of jointly executing scientific tasks. These will include the collection of sensor data which is distributed within the swarm agents and sensor measurements, time synchronization, and localization information will be exchanged between the agents. The German Aerospace Center (DLR) has designed a wireless communication system that is suitable for space exploration missions of this type where autonomous robots jointly explore unknown terrain on extraterrestrial worlds. The system enables data transmission as well as localization of the swarm agents by implementing a Physical Layer (PHY) and Medium Access Control (MAC) for unit-to-unit communication in the context of an ad-hoc network during in-situ space exploration missions. To allow the communication of swarm agents which are not in direct communication range, routing protocols are needed to relay packets of other agents.

This work presents a network simulation environment focused on in-situ space exploration missions for the evaluation of existing ad-hoc routing protocols. The simulation utilizes a wireless MAC using a Time Division Multiple Access (TDMA) channel access function implemented in this work resembling the DLR MAC on the network's nodes. Elevation data of the Moon's surface is taken into account for radio-propagation modeling in the simulation. Within this simulation environment 11 different experiment designs are implemented to evaluate the performance differences of the Dynamic MANET On-demand (DYMO), Destination-Sequenced Distance-Vector (DSDV), and Greedy Perimeter Stateless Routing (GPSR) protocols in operation on the TDMA MAC and a standard IEEE 802.11g MAC. Performance metrics are defined to compare the routing protocols utilizing the different MACs. The evaluation reveals observations like less stable operation of all routing protocols on the TDMA MAC and a bias introduced to the route establishment of the protocols by the builtin ordering. Further, the differences observed in operation of the individual routing protocols is discussed in details, such as DSDV always being capable of establishing the shortest route to its destination whereas the other routing protocols chose longer routes. Especially DYMO preferred staying on longer routes if the shortest route was not initially available. It is concluded that the DLR MAC will benefit from applications and routing protocols being aware of the TDMA scheme and incorporating the TDMA cycles into their operation to avoid additional waiting times or biases.

Contents

List of Figures

List of Tables

Acronyms

AODV . . . . . Ad hoc On-Demand Distance Vector Routing
API . . . . . Application Programming Interface

CPN . . . . . Colored Petri Net

DCAF . . . . . Distributed Channel Access Function
DLR . . . . . German Aerospace Center
DSDV . . . . . Destination-Sequenced Distance-Vector
DSR . . . . . Dynamic Source Routing
DT-FPN . . . . . Dynamic Topological Fuzzy timing high level Petri Net
DYMO . . . . . Dynamic MANET On-demand

GCMS . . . . . Gas Chromatograph and Mass Spectrometer
GDAL . . . . . Geospatial Data Abstraction Library
GPSR . . . . . Greedy Perimeter Stateless Routing

IAU . . . . . International Astronomical Union
IETF . . . . . Internet Engineering Task Force
IP . . . . . Internet Protocol
ISRU . . . . . In-Situ Resource Utilization

JUICE . . . . . Jupiter Icy Moons Explorer

LAN . . . . . Local Area Network
LOLA . . . . . Lunar Orbiter Laser Altimeter
LRO . . . . . Lunar Reconnaissance Orbiter
LUNAR . . . . . Lightweight Underlay Network Ad-hoc Routing protocol

MAC . . . . . Medium Access Control
MANET . . . . . Mobile Ad-Hoc Network

MARDI . . . . . Mars Descent Imager
Mastcam . . . . . Mast Camera
MTU . . . . . Maximum Transmission Unit

OFDM . . . . . Orthogonal Frequency Division Multiplex
OSG . . . . . Open Scene Graph

PDS . . . . . Planetary Data System
PHY . . . . . Physical Layer

SAM . . . . . Sample Analysis at Mars
SDK . . . . . Software Development Kit
SolO . . . . . Solar Orbiter
SOTDMA . . . . . Self-Organized Time-Division Multiple Access

TDMA . . . . . Time Division Multiple Access

UDP . . . . . User Datagram Protocol

WARP . . . . . Wireless Adaptive Routing Protocol

CHAPTER 1

Introduction

The rising interest in space exploration missions in which experiments on the surface of another planet or moon are conducted demands for new technologies to coordinate more complex mission scenarios [1]. Taking sensor measurements directly on site instead of observing from orbit is called in-situ space exploration. A variety of unique experiments has been proposed in the past for implementation in in-situ space exploration missions [2, 3]. With the landing of the Pathfinder spacecraft and the deployment of the Sojourner rover in 1997 the foundation for future space exploration missions has been laid. The rover traveled over 100 meters and conducted a multitude of experiments, investigating the martian dust settlement on the solar panel [4], the abrasiveness of martian soil, and the composition of rocks and soil found at the landing site [5]. Following the landing of Spirit and Opportunity in 2004, evidence was found for the former existence of liquid water on the surface of Mars during the in-situ exploration of the Opportunity rover at Meridiani Planum [6]. Apart from in-situ exploration on Mars there were other missions to extraterrestrial worlds, like the landing of the Huygens probe on the Saturn moon Titan. During the decent of the probe towards the surface of Titan, detailed imagery of the environment could be obtained along with measurements from several other instruments mounted on the probe. The in-situ visit on the surface of Titan revealed new insights on Saturn's moon including detailed measurements from the Gas Chromatograph and Mass Spectrometer (GCMS) which determined the composition of Titan's atmosphere [7]. Continuing on the success of the previous in-situ exploration missions to Mars, the Curiosity rover set wheels on the martian surface in 2012 and is continuously making new discoveries. The Sample Analysis at Mars (SAM) instruments provided new evidence for significant loss of atmosphere on the young Mars in the past [8]. During the martian summer on the southern hemisphere in 2015 the rover passed through the Bagnold Dune Field in the Gale crater where the Mast Camera (Mastcam) and Mars Descent Imager (MARDI) instruments were used to detect dune movement caused by surface winds [9].

These missions have proven to be a successful concept for in-situ space exploration. However, all these missions are utilizing a single rover unit for the in-situ exploration of extraterrestrial ground. Though, by utilizing a swarm of units a broader surface area can be investigated by distributing the swarm agents over the area of interest. As an example the agents could implement a distributed seismological investigation in the region by letting a

single agent emit acoustic waves in the ground while other agents are listening for these acoustic signals. By combining the measurements of each agent a geological reconstruction of the terrain can be generated. The swarm may repeat this exercise to enhance data resolution or the mapped area. To allow such interactions between agents of a swarm in a remote environment such as Mars or the Moon, a communication network capable of transmitting location, time, and sensor data is needed [10].

1.1 Motivation

The German Aerospace Center (DLR) has designed a wireless system that is well suited for missions where a swarm of autonomous robots jointly explores and investigates unknown terrain on extraterrestrial planets such as Mars. DLR proposes a concept for a wireless system jointly enabling communication and localization [11]. This concept defines the Physical Layer (PHY) and Medium Access Control (MAC) needed for a successful swarm communication during in-situ space exploration missions and allows direct unit-to-unit communication within an ad-hoc network. However, direct communication is often not possible due to obstruction in the line-of-sight or the sheer distance between the units of interest. As already pointed out by Zhang et al. [11], the use of a centralized solution for organizing the swarm's network is limiting the swarm mobility. To extend the approach for mobile swarm communication of DLR an ad-hoc routing protocol is needed where multi-hop communication is achieved by routing packets over several units instead of communicating directly with the destination unit. This extends the communication range of a single unit within the swarm to that of the whole network.

Such networks are very similar to communication networks used in situations like civilian emergencies found on earth [12] and a fitting candidate for routing packets through an extraterrestrial swarm network may therefore be found in an existing routing protocol already in use here on Earth. Conditions met in such environments include missing infrastructure such as the lack of energy supplies, base stations for communication, and roads. Connections within these networks are usually unstable and a routing protocol must be capable to cope with fast failing connections and the frequent establishment of new connections due to the movement in the network.

This work will investigate the applicability of existing routing protocols for robotic in-situ space exploration missions. The wireless communication system proposed by DLR will be integrated into a network simulation environment and several existing routing protocols will be evaluated in different experiments showing the viability of each routing protocol with respect to the mission-specific design of DLR's wireless communication system.

1.1.1 Theses

This work will investigate the feasibility of using well-established routing protocols in the domain of in-situ space exploration missions on Moon and Mars. It is expected that there exists at least a single routing protocol already in use on Earth which fulfills the requirements of in-situ space exploration missions as the operation of ad-hoc routing protocols in remote locations on Earth e.g. during civilian emergencies is similar to in-situ space exploration. Further it is investigated whether the localization and positioning information

retrieved by the MAC layer of DLR's communication system can be incorporated into existing routing protocols for potential benefits in route selection. To estimate the impact of DLR's communication system, the routing protocol performance will be compared to a standard IEEE 802.11 MAC. It is believed that specific physical constellations of swarm agents can create scenarios where DLR's system has disadvantages over a standard IEEE 802.11 MAC for conventional routing protocols. A suboptimal chain of hops on an unavoidable route can cause higher latencies when using DLR's system. These scenarios are discussed in detail in Section 3.2 and the impact of DLR's communication system on the performance of conventional routing protocols is analyzed in detail in Section 4.1.

1.2 Thesis Structure

The next chapter provides a brief overview on existing routing protocols for a variety of applications. Next, several approaches for verification of ad-hoc routing protocols are presented and a variety of in-situ space exploration mission designs are discussed and put in perspective to extraterrestrial swarm exploration missions. Chapter 3 describes the design choices considered during implementation of the simulation environment followed by a detailed discussion on experiment design and explanations on how routing protocols are tested against the special conditions met in DLR's communication system. The next chapter evaluates the results gained from the experiments discussed in the previous section followed by a conclusion and a short perspective on future investigations extending this work.

CHAPTER 2

Related Work

In the past a multitude of different routing protocols have been developed for a variety of applications. Many of them find implementation in Local Area Networks (LANs) whereas space exploration missions demand wireless solutions. Wireless networks divide into two types of networks: a centrally administrated wireless network with access points and a single router; and an ad-hoc network where each host within the network is capable of routing packets [13, 14, 15]. Ad-hoc networks are ideal for groups or swarms of wireless hosts which are constantly changing the topology of the network by physical movement and joining or leaving of hosts. Any central administration or fixed infrastructure usually found in other types of networks is not necessary [13, 16, 17]. Therefore, ad-hoc wireless networks are a promising candidate for establishing communication in a swarm of agents during remote planetary exploration missions [12].

While focusing on existing routing protocols in use today, a brief summary of said protocols is mandatory. In 1994, Perkins and Bhagwat [18] proposed a highly dynamic Destination-Sequenced Distance-Vector (DSDV) routing approach based on the Bellman-Ford routing mechanisms where each node maintains its own routing table with proactive route updates. Johnson and Maltz [13] presented the Dynamic Source Routing (DSR) protocol in 1996 with its subsequent publication as the experimental RFC 4728 in 2007 [19]. This protocol uses a reactive route discovery approach within the network which was found to be more energy efficient than proactive approaches. The protocol does not need the connectivity between two hosts to be bidirectional. The complete route for a packet is determined on the transceiver and placed in the packet's header. Each node involved in the route will transmit the packet to the next hop on the previously selected route until the packet reaches its destination. Following on energy efficient wireless networks, Intanagonwiwat et al. [20] proposed the use of a Time Division Multiple Access (TDMA) based MAC layer for energy efficient communication within sensor networks. In 1999, Perkins and Royer [14] presented the Ad hoc On-Demand Distance Vector Routing (AODV) routing protocol which assembles routes on-demand and therefore belongs to the class of reactive routing protocols. It requires symmetric links between neighboring nodes to establish a route. In 2001, Hong et al. [12, 21] searched for a suitable and energy efficient routing protocol for use in a martian sensor network. The requirements for ad-hoc routing protocols for data centric sensor networks in planetary exploration missions were collected. Terrestrial wireless, multi-hop ad-hoc

networks like used during civilian emergencies or group networking were identified to be functionally similar to martian sensor and rover networks. When selecting a routing and broadcasting strategy the additional energy consumption of individual nodes within the network is a critical issue as nodes which are heavily involved in packet forwarding tend to consume more energy and may eventually die due to drained batteries. Distributing the packet forwarding tasks equally over all nodes in the network is therefore seen to be a crucial part of a routing protocol. Hong et al. proposed an AODV based routing protocol with adjustments to the flooding scheme and route selection by respecting a passively distributed energy level of neighboring nodes. Following on the establishment of AODV in several applications, the Internet Engineering Task Force (IETF) accepted the AODV routing protocol as experimental RFC 3561 [22] in 2003. The Dynamic MANET On-demand (DYMO) IETF draft overcomes the protocol overhead of the route discovery in AODV and acts as a successor of AODV. It aims for a simpler design to reduce implementation effort and protocol overhead. DYMO possesses a path accumulation function which integrates source routing behavior into the protocol where a node gains knowledge of the network without initiating a route request on its own [23].

A different approach is implemented in the Greedy Perimeter Stateless Routing (GPSR) protocol by Karp and Kung in 2000 [24]. This protocol solely bases routing decision on the geographic position of a node without regard to latency or hop count. Each node has knowledge of its direct neighbors and their geographic position through periodic broadcast beacons containing the Internet Protocol (IP) address and position. Beacons are piggy-backed on all data packets of a node to reduce the overhead produced by proactive beaconing. GPSR does not respect a nodes altitude and assumes nodes to reside on a flat plane. Links between nodes are expected to be bidirectional. The protocol uses a greedy packet forwarding mechanism where packets are forwarded to the node closest to the position of the destination node. If all neighboring nodes are further away from the destination than the current node, the packet is routed to the next node in counter-clockwise direction and enters a perimeter mode. This routes the packet around an area where a direct connection to the destination does not exist until a node is reached which is closer to the destination than the node where the greedy routing last failed. The GPSR routing protocol uses a planar graph of the network topology for routing a packet in perimeter mode. As ad-hoc networks tend to build topologies which are not compatible with a planar graph, the network topology must be planarized. The routing protocol removes connections between nodes to eliminate crossing links in the network graph. This is done locally on each node in a distributed manner. The planar property in conjunction with the counter-clockwise routing rule is necessary to avoid loops when routing in perimeter mode.

In 2002, Ramanathan and Redi [16] suggested to combine movement information of nodes retrieved from other sensors with the routing information from the network layer through the utilized routing protocol. This idea was implemented in a proposal by Trajanov and Filiposka [17] where a combination of topology information and a social network running on an ad-hoc network is used to link people in a social graph which are close to each other. This is achieved by mapping the physical topology of hosts within the network to people participating in the social network. The same idea is applied by Zhang et al. [11] in the domain of space exploration where localization information from the physical layer can be incorporated into applications running on the network hosts. The self-organized TDMA channel access on the MAC layer presented in this work by DLR can exploit the radio

signals within a swarm of agents to retrieve positioning information of nodes.

2.1 Evaluation and Simulation Strategies

Based on the formulation of aforementioned routing protocols, several approaches got discussed on how to validate the correct operation of a routing protocol as well as the viability of an approach for a specific application. Kum et al. [23] compared the performance of the AODV and DYMO routing protocol by simulating a virtual environment of 50 nodes within a rectangular flat space. Throughput, routing overhead, and the average packet size for routing packets were measured. It was clearly shown the DYMO reduces the protocol overhead when compared to AODV. However, AODV achieved a higher throughput with frequent movements in the network as the source routing approach of DYMO causes more route failures.

Xiong et al. [25] describe a different approach where formal verification is used for the evaluation of AODV. The approach for models and simulates the AODV routing protocol using Colored Petri Nets (CPNs). They identified unambiguity, completeness, and functional correctness of the utilized routing protocol to be the crucial part for ensuring a successful application of a Mobile Ad-Hoc Network (MANET). The work proposes a topology approximation mechanism for modeling the CPN to address the continuous movement of nodes and the concomitant changes of the network's topology. In 2004, Xiong et al. extended the approach for using CPNs for the verification of MANETs with the proposal of Dynamic Topological Fuzzy timing high level Petri Nets (DT-FPNs). This addresses the issue of modeling the dynamic nature of MANETs where nodes are frequently moving in and out of the transmission range of other nodes and is a crucial part in the verification of the reactivity of a routing protocol. In 2008, Espensen et al. [26] presented another verification technique for the DYMO routing protocol by utilizing a CPN model. The correctness of the routing protocol is validated by using a state space exploration approach. The utilized model covers scenarios with static topology and symmetric reliable links without packet loss. Each scenario contains a single route request among two to four nodes per network where no node is disconnected from the network. The model covers the mandatory parts of the DYMO routing protocol and revealed 7 issues in the specification which were resolved in later versions of the DYMO protocol.

A different approach for formal verification of ad-hoc routing protocols is presented by de Renesse and Aghvami in 2004 [27] where the SPIN model checking tool is used for formal verification of the Wireless Adaptive Routing Protocol (WARP). A similar strategy is implemented by Wibling et al. [15] where a non-interactive strategy for automatic verification of MANET routing protocols is presented. The reactive Lightweight Underlay Network Adhoc Routing protocol (LUNAR) has been chosen for a case study due to its low complexity where the protocol is verified with the SPIN model checker and the `UPPAAL` model checking framework. The case study revealed no flaws in the LUNAR specification and the routing protocol is considered to work correctly.

2.2 In-Situ Space Exploration Mission Designs

Future in-situ space exploration mission designs possess a multitude of variations in their implementation due to differing mission goals and objectives. The Jupiter Icy Moons Explorer (JUICE) will encounter extremely cold temperatures down to $-200\,°C$ whereas the Solar Orbiter (SolO) will exercise direct remote sensing of the Sun at a closer distance then ever before hence experiencing temperatures up to $520\,°C$ [28]. In 2005, Fong and Nourbakhsh [29] proposed to support human space exploration with human controlled or autonomous robots. Astronauts visiting the surface of other celestial bodies will utilize wireless communication systems to transmit commands to in-situ robots. These robots will provide requested data back through the same communication channel. If a multitude of robots is deployed during such missions, inter-robot communication becomes necessary for efficient coordination [29]. In order to extend the communication range for commands from a human operator, the commands have to be relayed over several robots to inform a distant agent about new tasks [11]. If human support is not feasible due to health risks or overall mission cost, an autonomous system as described by Ceballos et al. [30] can be utilized instead of human operators. This system provides adjustable levels of autonomy through a robust and verifiable autonomous controller. The approach could be extended to support the control of an autonomous swarm in a remote extraterrestrial environment. The vehicles utilized in such a swarm can differ significantly depending on the celestial body of deployment. In 2017, Gao and Chien [3] provided a brief overview of vehicle concepts proposed for implementation in space exploration missions, including a helicopter similar to the recently successfully deployed rover Perseverance's companion helicopter drone Ingenuity embedded into the Mars 2020 mission. Other vehicles include a Mars airplane, an aerobot suitable for the exploration of Titan, and underwater vehicles for in-situ visits to the Jupiter moon Europa.

Using autonomous robot systems lowers the cost of space exploration missions. In-Situ Resource Utilization (ISRU) is further extending the use of robot systems to lower the cost of space exploration missions. It investigates the extraction of materials available at the site of scientific interest to support the mission with required resources like fuel or if human operators are involved on site, water or oxygen [2]. Sacksteder and Sanders [31] describe methods for extracting oxygen from lunar regolith. The lunar poles are especially of interest as they possess significantly more oxygen and hydrogen than the equatorial region of the Moon. In 2018, Sanders [32] proposes to utilize in-situ fueled hoppers enabling access to a broader area for scientific experiments with the ultimate goal of making these missions earth-independent. The same year, Lin et al. [33] published China's plans for ISRU in combination with a lunar station and several in-situ missions to Mars also including sample return as well as plans for a preliminary research station at the Moon's south pole. In 2020, Chen et al. [34] presented plans for an affordable and sustainable interplanetary space transportation system for Mars. The use of ISRU systems and storage for acquired resources were identified as critical infrastructure for operations in space. The benefit for utilizing ISRU during human mars exploration was investigated and concluded that direct ISRU on Mars in preferable over intermediate ISRU on the Moon as deployment costs for ISRU systems on the Moon will not pay off.

CHAPTER 3

Thesis Contribution

This work implements a simulation environment for the evaluation of ad-hoc routing protocols within the context of the swarm navigation system presented by the DLR [11]. The capabilities and restrictions of the experiments conducted in that simulation environment will be discussed as well as the viability of the simulation results. Furthermore, an approach for validating the applicability of several existing routing protocols in an ad-hoc network implementing DLR's communication system will be presented. A number of experiments will be described which are implemented in the simulation environment. The results of said experiments are discussed in the next chapter.

3.1 Implementation

This chapter provides implementation details and design choices considered during simulation environment development for the evaluation of ad-hoc routing protocols in the scope of in-situ space exploration missions. The simulation is hosted within the `Omnet++` discrete event simulator in conjunction with the `INET` model suite for wired, wireless and mobile networks [35].

3.1.1 The Physical Environment

In-situ space exploration missions are hosted in a variety of different environments, ranging from the cold and thick atmosphere of Titan to the barren landscape of the Moon. This work focuses on in-situ space exploration missions on the Moon. The inclusion of characteristics found during such missions needs to be investigated. The Moon possesses a lot of environmental differences when compared to Earth where the characteristics relevant to routing protocols are radio-signal obstructions and interference resulting from radio-propagation along the terrain. Interference and noise on the signal created by e.g. increased levels of radiation are expected to be regarded by the underlying MAC and PHY. Instead of placing obstructions in the scene manually the `INET` and `Omnet++` frameworks provide the possibility to integrate the *Open Scene Graph (OSG)* 3D graphics toolkit. This toolkit enables the use of a three-dimensional scenery inside the simulation. With the help of the `osgEarth`

geospatial 3D mapping engine and Software Development Kit (SDK) a variety of terrain models can be included into an INET simulation. The terrain models of an osgEarth scene use elevation data to reconstruct parts of the surface of a celestial body. This elevation data is used in INET by several error models to calculate interference and obstruction of a signal. The terrain models can therefore be used to implement realistic mission scenarios by accounting for the elevation characteristics found in in-situ space exploration. Aside from the special features of DLR's MAC and PHY discussed in Section 3.1.4 the use of realistic elevation models tailors the simulation towards specialization on in-situ space exploration missions.

Within the simulation the Lunar Orbiter Laser Altimeter (LOLA) data of the Lunar Reconnaissance Orbiter (LRO) is primarily used to provide elevation data of the Moon's south pole, particularly the Boguslawsky crater at the very south of the earth-facing (near side) of the Moon which is proposed as a landing site for the upcoming *Luna 25* mission [36] and the Schrödinger crater with its rocky terrain at the far side of Moon. The Boguslawsky crater. The LOLA data of the LRO provides a high-accuracy topography mapping of the whole Moon [37] which is prepared in several derived data sets, one of which is an elevation map of the whole Moon. Data from the south pole of the Moon is used within the simulation to provide an accurate terrain model with osgEarth.

The LOLA data is provided in the Planetary Data System (PDS) format in version 3. The data is imported into the simulation with the help of osgEarth and the Geospatial Data Abstraction Library (GDAL). While implementing the integration of OSG and osgEarth into the simulation several technical challenges arose, mostly due to misuse of a newer osgEarth Application Programming Interface (API) within Omnet++ and INET. Additionally, all frameworks had difficulties to correctly process terrain-data for other celestial bodies except Earth. This was caused by the Moon having a different reference ellipsoid with differing equatorial radius and polar semi-minor axis. The Moon's reference ellipsoid is defined by the International Astronomical Union (IAU) in the Moon2000 projection. Whereas most of the OSG and INET code is erroneously using the WGS84 projection of the Earth's ellipsoid for placing and positioning scene objects, OSG and osgEarth were mostly capable of handling other celestial bodies apart from Earth. A visual bug in osgEarth's sky shader caused the Moon to disappear when manually checking for correct mapping of terrain data during development. As this issue is not present in the osgEarth version 2.10 this version was selected to host the INET simulations. The projection issues in OSG and INET were fixed by retrieving the reference ellipsoid used for projection through osgEarth instead of using a hard-coded WGS84 projection and enabling the use of coordinates within this reference ellipsoid for positioning scene objects.[1] Additionally, the implementation of the GPSR protocol has been altered to use the distance and angle calculations of the osgEarth coordinate system as the default implementation was incompatible with other coordinate systems.

The LOLA data contains a pre-scale factor which defines each pixel inside the data-set to be half as high as the elevation suggests. Unfortunately, this pre-scaling is not accounted for by osgEarth or GDAL while importing the LOLA data-set. This leads to the terrain's elevation being twice as high as seen in reality. As the absolute height of the terrain elevation is not important for the experiments, but using realistic terrain shapes to create obstructions which are expected in real space exploration missions, this error persists in the

[1] https://github.com/omnetpp/omnetpp/pull/851

final simulation and the source of the error has not been investigated.

3.1.2 Modeling Obstructions in the Line-of-Sight

The primary tool for integrating obstructions and other environmental characteristics into simulations in the `INET` framework is the obstacle loss model [38]. The obstacle loss model can place several obstructions with different materials and shapes into a simulation to affect the signal propagation of transmissions. Unfortunately, it does not provide a straightforward method for the integration of data-sets like the LOLA data. As path loss models possess the ability to incorporate OSG ground models within `INET` [38], path loss models were chosen in favor of obstacle loss models to include the effects of the terrain in the simulation.

There exist several different path loss models in `INET` which are responsible for simulating the effect on the strength of radio signals while propagating from the transmitter to the receiving end of a transmission. The models possess variable accuracy and along with that also varying computational cost. By using ground models from data-sets like the LOLA data insights can be gained regarding the specific challenges for in-situ space exploration missions. Although path loss models are usually not included in simulations for the evaluation of routing protocols, they are included in this work to accommodate the obstruction and interference characteristics of in-situ space exploration missions into the simulation.

Not all path loss models of the `INET` framework support the integration of ground models. As documentation on that matter was lacking at the time of writing, the existing path loss models of INET were studied for references to the `osgEarth` API for retrieving information about the ground shape. The `TwoRayGroundReflection` [39] path loss model was found to be capable of integrating a ground model from the physical environment into the signal propagation. This path loss model assumes a flat ground between the elevation points of sender and receiver and therefore does not contain a free line-of-sight check. This results in false successful communications within the simulation when the line-of-sight is obstructed by hills or rocks. To counteract this, a simple line-of-sight check has been added to the

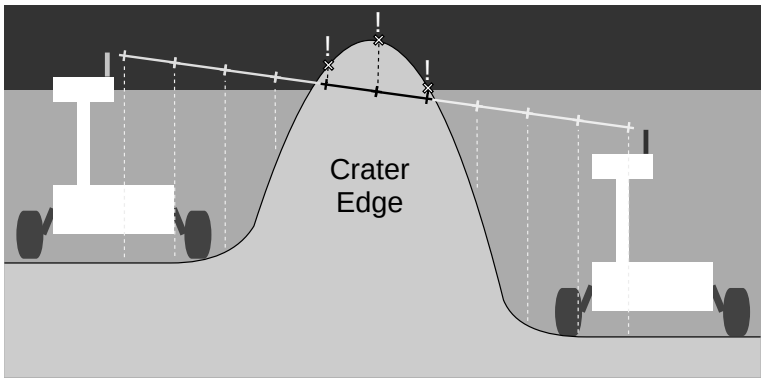

Figure 3.1: Steps on the line-of-sight with detected collision on a crater edge by comparing ground elevation with the altitude of the step on the line-of-sight

`TwoRayGroundReflection` prior to the path loss calculations. This approach is sufficient to evaluate routing protocols in an environment with obstructions created by crater lips or rocky terrain but may lead to inaccurate results in other simulations where the exact power loss and diffraction created by the terrain is relevant to the simulation.

The line-of-sight model integrated into the `TwoRayGroundReflection` uses discrete steps on the line-of-sight between the transmitter and receiver of a transmission (see Figure 3.1). Each of these points is then checked for collision with the terrain of the ground model by comparing the altitude of the ground with the altitude of the point on the line-of-sight. If the point is below the altitude of the ground, the line-of-sight is considered obstructed and a complete signal loss appears.

The amount of points on the line-of-sight has great impact on the accuracy of this check. By default, the check uses a resolution of 2 points per meter. This resembles approximately the resolution of the terrain data provided by `osgEarth` through the LOLA dataset. The resolution is additionally clamped to a maximum of 1000 points and a minimum of 1 point per communication pair. A maximum has been chosen to reduce the computational cost for transmissions over long distances.

With this line-of-sight model it is possible to simulate obstructed transmissions between a communication pair at the crater edge or on rocky terrain.

Algorithm 1 Pseudocode for line-of-sight collision detection

```
1: distance = Calculate distance between transmitter and receiver position
2: steps = Twice the computed distance but at least 1 and at most 1000
3: for each step do
4:     Calculate offset along the line-of-sight regarding the current step
5:     Retrieve altitude at calculated offset on the line-of-sight
6:     Retrieve altitude at calculated offset on the ground
7:     if Ground altitude ≥ line-of-sight altitude then
8:         Quit calculation and emit full path-loss due to obstructed line-of-sight
9:     end if
10: end for
11: No obstruction detected, continue with ground reflection calculations
```

3.1.3 Choosing an Analog Model

The analog model of the simulation determines the representation of radio signals within the simulation. It controls the transmission, propagation, and reception of radio signals according to one out of several analog signal models [40]. Choosing an appropriate analog model for the simulation can have great impact on the simulations runtime and the accuracy of the results. In `INET` three models for representing an analog signal exist: the *Unit Disk* analog model, the *Scalar* analog model, and the *Dimensional* analog model.

The *Unit Disk* analog model is the most simple analog model in `INET`. It is utilizing three parameters to represent a signal within a circular disk around the sender's position: communication, interference, and detection range [40]. Further inspection of the *Unit Disk*

analog model revealed that path loss models are not supported in combination with this analog model. As described in Section 3.1.2 `INET` path loss models are used to integrate the environment into the signal propagation during a transmission. As the ultimate goal of this thesis is to evaluate the performance of well-established routing protocols within an environment typically found in in-situ space exploration missions, the lack of a path loss model hinders the adjustment of the simulation to properly picture such an environment.

The *Scalar* analog model is using a single scalar value to represent the signal power of transmissions to calculate the probability of a successful reception at the receiver by applying attenuation and noise. A transmission is composed of a center frequency and a bandwidth which are modeled as flat signals in frequency and time [40]. This makes realistic simulation of interference between several different signals with potentially different technologies impossible. As simulating interference between several wireless technologies is not needed for evaluating the performance of ad-hoc routing protocols on a single wireless technology, this restriction is not relevant for this work.

In contrast to the *Scalar* analog model, the *Dimensional* analog model uses a two-dimensional function to model arbitrary shapes in frequency and time. Attenuation, interference, and noise are all simulated with respect to frequency and time. This model is therefore capable of simulating interference between multiple signals of different shapes withing the two-dimensional frequency and time domain [40]. As previously discussed this is not needed for the evaluation of ad-hoc routing protocols and therefore serves no benefit to this work.

At the time of writing the *Scalar* analog model is the only analog model which is compatible with the *TwoRayGroundReflection* path loss model. To avoid additional work for porting the *TwoRayGroundReflection* to other analog models, the *Scalar* analog model has been chosen to serve as the analog model for the simulations in this work.

3.1.4 Implementation of the TDMA MAC

This work is centered around the swarm technologies developed by the DLR for the use in future space exploration missions. The core technology proposed by the DLR in preceding works [10, 11] is the wireless communication between agents of the swarm. The communication is based on a Self-Organized Time-Division Multiple Access (SOTDMA) technique where exclusive access to the communication channel is granted to a single agent within a time slot. The system is self-organizing in a way where the number of total time slots available to the agents is adaptive to the number of agents within communication range. The system ensures that each agent of the swarm has access to exactly one TDMA time slot through static configuration. This ensures the absence of any interference created by collisions on the communication channel. The adaptive nature of the TDMA slot configuration allows the application of the system in scenarios where the topology of the swarm is continuously changing. This includes the segmentation of the swarm into multiple smaller swarms and the joining of multiple swarms into a single all-encompassing swarm. The limits of the system are defined as a maximum network update rate of 100 Hz for 20 agents, resulting in a minimal slot duration of 500 µs for each agent. The maximum movement speed of the agents is defined as $100\,\mathrm{km\,h^{-1}}$. The system modulates signals with Orthogonal Frequency Division Multiplex (OFDM) [11].

The main difference of this technology to the *IEEE 802.11* MAC which is included by

default in the INET framework (version 4.2.0) is the TDMA channel access. As the crucial point in the evaluation of routing protocols for this system is the behavior observed from the outside, it was decided to use the included *IEEE 802.11 MAC* as a basis for the inclusion of DLR's MAC in the simulation. The channel access of INET's *IEEE 802.11* MAC has been altered and rewritten to match the TDMA scheme. It controls when a node is allowed to transceive a signal on the channel and when not. Whilst the *IEEE 802.11* MAC commits great effort into the handling of collisions on the radio channel e.g. through the management of a contention window, the TDMA MAC does not need this collision management as it is impossible to create collisions on the channel due to the nature of TDMA. To avoid extensive changes in INET's *IEEE 802.11* code, the contention window length has been set to 0 for the TDMA MAC. This leads to the contention window being ignored. However, this allows changing the channel access method within the same MAC code and enables direct comparison between a standard *IEEE 802.11* MAC and the TDMA MAC. This is achieved by enhancing the *IEEE 802.11* MAC of INET to host different channel access methods.

3.1.5 TDMA Channel Access

The essence of this work is to evaluate the viability of several routing protocols for space exploration missions with the underlying TDMA MAC concept implemented by DLR. A simulation environment is created to allow the evaluation of the routing protocols. In order to yield meaningful results from the simulation the required level of realism for the simulated MAC has to be given adequate consideration. Specifically, the TDMA channel access method has to be implemented in a way that resembles the core functionality of the DLR's TDMA scheme. The differences of the TDMA scheme in contrast to the *IEEE 802.11*'s default implementation must appear in the simulation and have an influence of the routing protocol. Therefore it is important to represent the *behavior* of the TDMA in the simulation and not an exact physically accurate model of the MAC and PHY.

This is achieved by implementing a three-state logic in the TDMA channel access where the channel access for each node can either be `Idle`, `Waiting`, or `Owning`. The module ensures that only a single node has an `Owning` within a network. All other nodes initially switch to the `Idle` state and transition to `Waiting` if channel access was requested by the upper layer. The channel access request is queued until the node enters its next TDMA slot. The `Waiting` state has no effect on the organization of TDMA slots within the network but is only an internal marker to tell the MAC that there is data available for transmission. If there is no data available to send on a node which enters the `Owning` state then simply no transmission is done. For synchronization of the TDMA slots the global simulation time is used in every node. Therefore, clock skew of the nodes is not accounted for in the simulation and assumed to be a solved problem which is invisible to a potential routing protocol. Furthermore, the packets sent on the MAC are not scheduled on-demand to fully utilize an `Owning` slot. Instead, the simulation is configured in a way that fits packets into TDMA slots by choosing proper delays and packet sizes in the application layer. However, as pre-scheduling is not always possible for all routing protocols, a margin of one millisecond has been introduced before an `Owning` TDMA slot ends where no further packets are accepted for transmission from the upper layer. Instead, those packets will be queued for the next TDMA cycle. This ensures that no transmission is possible while the channel access transitions from `Owning` to `Idle`. The margin is configurable to allow adjustment for different packet sizes in different

Ground model	`osgEarth` ground with LOLA/MOLA data, see Section 3.1.1
Coordinate system	OSG geographic coordinate system, see Section 3.1.1
Analog model	Scalar analog model, see Section 3.1.3
Radio medium	IEEE 802.11 scalar radio medium, see Section 3.1.3
Path loss model	Modified `TwoRayGroundReflection` with, see Section 3.1.2 line-of-sight check
Visualizer module	If visualization of the simulation is enabled (e.g. for development) a custom enhanced `osgEarth` visualization module is used containing fixes for differing projection of the terrain on the Moon
MANET routing module	Custom MANET routing module for all nodes which allows exchange of the channel access function (e.g. DCAF and TDMA), see Section 3.1.4

Table 3.1: Models included in the simulation and their non-standard adjustments in INET

simulations.

3.2 Experiments

Continuing on the setup of the simulation environment in the previous section, the design of the experiments conducted in said environment will be discussed in depth in the following section. The experiments are categorized into five experiment groups with differing experiment complexity: the *simple experiments* group, the *basic agility experiments* group, the *advanced experiments* group, the *generated experiments* group, and the *alternative route experiments* group. The experiment setup and research focus will be thoroughly described for each experiment group in the following sections.

3.2.1 Simple Experiments

Ad-hoc routing protocols have to cope with a multitude of complex situations. In the past, the design of ad-hoc routing protocols spent great thought on the avoidance of errors like routing in loops in a variety of rare and complex scenarios (see Chapter 2). However, it is equally important to assess the capabilities of a routing protocol in the most simple scenarios, e.g. the time it takes the protocol to establish a connection (route) to a second node in a simple two-node network setup along with the number of packets lost. The *simple experiments* group is designed to test the performance of routing protocols where a routing protocol is essentially not needed due to a direct connection between nodes where no routing over other nodes is necessary. This will reveal the overhead introduced by a routing protocol with respect to additional packets as well as the aforementioned route establishment latencies and the achieved throughput. Additionally, this experiment group

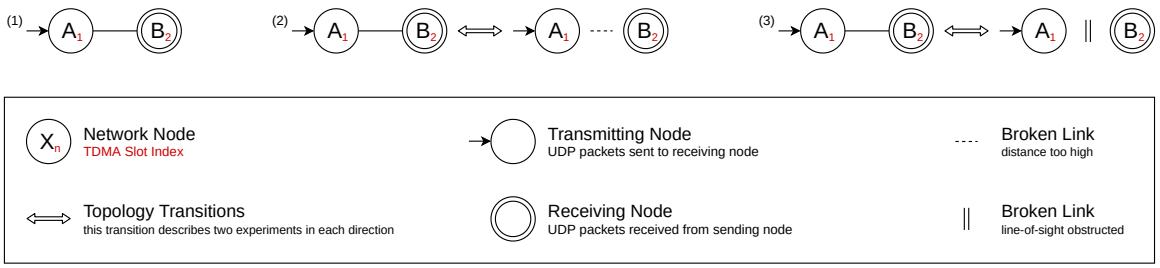

Figure 3.2: The setup of the *simple experiments* group along with a legend describing the graph semantics.

serves as a reference for more complex experiments.

The *simple experiments* group consists of three basic experiment layouts (see Figure 3.2) whereas *(2)* and *(3)* each describe two experiments for each direction of the described topology transition resulting in five distinct experiment setups in total. The experiment *(1)* describes a completely static setup without any movement and a stable connection between the two depicted nodes. This experiment will reveal the minimal overhead produced by a routing protocol. The experiments *(2)* and *(3)* focus on basic topology changes. Experiment *(2)* depicts a slow graduate change in topology where a complete loss of connectivity is created by a linear movement of the node Ⓑ. The experiment is conducted in both directions where Ⓑ steadily approaches Ⓐ and secondly steadily departs from Ⓐ. The experiment *(3)* focuses on the rapid change of topology induced by a line-of-sight obstruction of the nodes Ⓐ and Ⓑ. This is created by a constant movement of both nodes over a rough terrain at the Moon's south pole near the Schrödinger crater at the far side of the Moon. The distance between the nodes is constant throughout the experiment. The rapid change in connectivity is created by a rock moving into the line-of-sight due to the movement of the two nodes. This experiment is conducted in both directions where the experiment begins with the rock blocking the line-of-sight of the two nodes where a linear movement of the nodes frees the line-of-sight later into the experiment. Secondly, the experiment begins with a free line-of-sight where a movement of the nodes towards the rock leads to an obstruction of the line-of-sight.

As discussed in Chapter 2, energy consumption is of great importance for in-situ space exploration missions. Lowering the packet overhead of a routing protocol has direct impact on the energy consumption of a node. The less data is transmitted from the node, the less the physical radio is utilized resulting in less energy consumption. Apart from energy consumption, the additional latency for transmitting a packet to its destination introduced by a routing protocol is of great interest for the design of applications running on the ad-hoc hosts. Of particular interest is the latency between the creation of an application packet and the start of its transmission on the physical radio of the sender. This latency describes the delay created by the establishment of a route to the destination. While ideally this latency should be constant in order to achieve realtime capability, it is expected that this latency is very dynamic for protocols implementing reactive routing. A constant route establishment latency is (if at all) only expected in proactive routing protocols or if a number of preconditions are met, like an up-to-date route cache induced by frequent messages on

a given route in a source routing based protocol. It is expected that energy conserving routing protocols perform rather poor with respect to the route establishment latency as these two properties contradict each other. Additionally to the latency created prior to the transmission of an application packet on the physical medium, further latency can be created by the routing protocol determining the path to the destination en route like seen in greedy routing protocols such as GPSR. The packet loss observed in the experiments can indicate the ability of a routing protocol to quickly adapt to a new topology. The lower the packet loss, the quicker the routing protocol recognized the appearance of a new route. This is especially true in a simulation environment where packet loss induced by interference with other signals is eliminated by experiment design. The overall data throughput measured in experiment *(1)* will be used in later experiments to compare the performance in more complex topologies.

In all experiments, an User Datagram Protocol (UDP) application on the sender sends packets to another UDP application on the receiving node. The packets are sent in intervals of 20 ms with a specific packet size depending on the simulation runs configuration. The packets are sent in the direction of the TDMA slot indices. This is especially relevant for networks containing more than two nodes. Sending a packet along the direction of TDMA slot indices resembles a best-case scenario where a packet can be immediately forwarded to the next hop as nodes enter their TDMA slot directly after reception of the packet. This allows immediate forwarding or transmission of a response. However, responses traveling over more than a single hop lead to the packets traveling contrary to the TDMA slot indices and therefore resembling a worst-case scenario. Packets sent from the destination node are expected to be routing protocol packets which are needed for a route establishment. As the *simple experiments* group only contains experiments with networks containing two

Parameter	**Values**
Wireless MAC	DLR TDMA MAC, IEEE 802.11 MAC
Deployed routing protocol	DYMO, GPSR, DSDV
Packet size sent from transceiver	$\frac{1}{2} \cdot MTU$, $1 \cdot MTU$, $2 \cdot MTU$
TDMA slot length per node	500 µs, 1 ms, 10 ms with 128 B, 256 B, 2048 B MTU
Physical environment	Rocky terrain in Schrödinger crater
Velocity of node Ⓑ in *(2)*	$5\,\mathrm{m\,s^{-1}}$, $10\,\mathrm{m\,s^{-1}}$, $20\,\mathrm{m\,s^{-1}}$
Obstruction time in *(3)*	After 10 s, 30 s, and 60 s into the simulation
Frequency of application packets	Every 20 ms
Duration of experiments	80 s
Repetitions of experiments	10 repetitions for each parameter combination

Table 3.2: Simulation parameters for the *simple experiments* group. Scenarios are generated by combination of all parameters resulting in 702 distinct scenarios.

nodes, this effect will not be observable within this experiment group. Experiment groups composed of networks with more nodes are expected to show this effect.

Each experiment is running in several scenarios with different parameterization as depicted in Table 3.2. The experiments are conducted with the TDMA MAC by DLR as well as a standard IEEE 802.11g MAC utilizing a Distributed Channel Access Function (DCAF). The DYMO, GPSR, and DSDV routing protocols are tested in all the experiments. The size of the packets sent by the UDP application is adjusted relative to the Maximum Transmission Unit (MTU) of the MAC layer in three different ways. Choosing different packet sizes depending on the MTU size leads to fragmented packets or packets with spare bytes for additional information potentially attached by the routing protocol which has an effect on the overall utilization of the links. The TDMA slot length is adjusted to reveal the impact of longer TDMA cycles on the route establishment latency. The TDMA slot length is coupled with the MTU of the MAC as longer slot lengths allow for larger packets to be transmitted within a single TDMA slot. Therefore, the MTU is adjusted along with the slot length. In simulations running the IEEE 802.11g MAC the slot length has no effect, but by configuring the according MTU on that MAC the results from both MACs can be compared. It is expected that the route establishment latency changes along with the selected slot length. Furthermore, the movement speed and obstruction time is altered in experiments *(2)* and *(3)*. A routing protocol might react differently depending on how long a stable connection has already been established. The positioning and movement of the nodes within the experiments is statically configured with only a single sender and a single receiver in each scenario. Therefore no interference of radio signals is expected within the simulation.

In order to measure the packet overhead produced by a routing protocol, the packets on each node are counted with regard to the origin of the packet. The packets originating in the routing protocol itself can then be put into perspective to each sent UDP data packet. This allows estimating the overhead produced by the routing protocol per data packet sent by the application. When putting the packets associated to the routing protocol in proportion to other packets within a given time frame, the overhead of the routing protocol can be visualized over time. As a packet passes through the several layers of the network stack, the route establishment latency can be easily measured by comparing the time at which a UDP packet is created in the application and its arrival in the MAC layer. When comparing the number of packets sent on the sending node and the number of packets received at the receiving node, the packet loss is calculated. The number of packets received on the receiving node within a certain time frame yields the throughput achieved over the connection.

The insights expected by this experiments include how the overhead and packet loss compares between the individual routing protocols as well as how the overhead and packet loss change with parameters like the packet size, TDMA slot length, and velocity of the nodes. Furthermore, these experiments will show how the latency and throughput are affected by the changes to these parameters, especially when comparing the experiments *(2)* and *(3)* to *(1)*.

3.2.2 Basic Agility Experiments

In real world applications ad-hoc networks usually span more than two nodes as previously depicted in the *simple experiments* group. The *basic agility experiments* group focuses on minimal networks where routing can be used to establish communication. This group checks the ability to select alternative routes upon a change in network topology. This is expected to happen frequently during in-situ space exploration missions. These experiments necessitate the adaptation to new topologies and make the basic agility of a routing protocol observable.

Figure 3.3: The setup of the *basic agility experiments* group. The legend for this graph is included in Figure 3.2.

The layout of the experiments is visualized in Figure 3.3. The experiments possess a network of three fully connected nodes where two possible connection failures are depicted in the experiments *(4)* and *(5)*. Although, in a fully connected network, direct communication between two nodes is possible, a routing protocol can still utilize the third node for the establishment of an alternative route. The experiment *(4)* depicts a scenario where a third node which is not essentially needed for successful communication between sender and receiver loses connection to the network. Proactive routing protocols are expected to notice this change of topology whereas reactive protocols are expected to ignore this change. The same behavior is expected when executing the experiment in the opposite direction. The movement of node Ⓑ is orthogonal to the line-of-sight of Ⓐ and Ⓒ. This results in Ⓑ moving towards the nodes Ⓐ and Ⓒ whereas in the second scenario Ⓑ distances itself from Ⓐ and Ⓒ. The fifth experiment creates a situation where the routing protocol is forced to establish a route over node Ⓑ as the direct connection between sender and receiver vanishes due to an outward movement of Ⓐ and Ⓒ. This leads to the full mesh network transforming into a chain of nodes where the optimal route is the one visiting all nodes in the network. The opposite direction of this experiment establishes a full mesh network from a chain by inward movement of nodes Ⓐ and Ⓒ.

The agility of a routing protocol can be expressed as the time in which the protocol adapts to new topologies and thereby minimizing route establishment latencies and packet loss. By measuring the time it takes a packet from creation in the application to processing in the transceivers MAC, a route establishment latency can be described. A low latency yields faster adoption to new topologies and thereby better agility. Counting the successfully received packets in the receiving application and putting this into proportion to the created packets in the sender application yields the overall packet loss. As the applications are utilizing UDP, the application packet loss will increase if no route is established between sender and receiver. However, as the experiments include situations where there is no physical connection possible between the sender and receiver, the packet loss metric

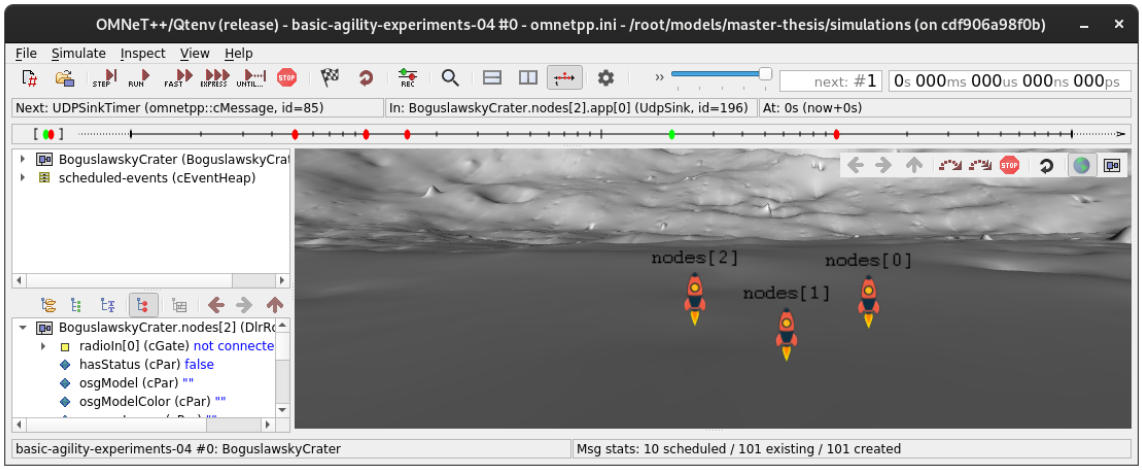

Figure 3.4: The `osgEarth` visualization of experiment *(04)* as seen in the graphical user interface of *Omnet++*.

compares the application packets which are actually transmitted on the sending node with the packets received on the receiving node. This yields the packets lost due to invalid or unstable routes. The exact moment in which the routing protocol transitions from one route to an alternative route within the described experiments can be depicted by observing the amount of hops on the currently active route. This hop count includes the number of nodes a transceived packet has visited until reception at the destination node.

The *basic agility experiments* group utilizes the same parameterization as the *simple experiments* group and extends the insights to dynamic topologies which require alternative

Parameter	**Values**
Wireless MAC	DLR TDMA MAC, IEEE 802.11 MAC
Deployed routing protocol	DYMO, GPSR, DSDV
Packet size sent from transceiver	$\frac{1}{2} \cdot MTU$, $1 \cdot MTU$, $2 \cdot MTU$
TDMA slot length per node	500 µs, 1 ms, 10 ms with 128 B, 256 B, 2048 B MTU
Physical environment	Flat terrain in Boguslawsky crater
Velocity of nodes	$5\,\mathrm{m\,s^{-1}}$, $10\,\mathrm{m\,s^{-1}}$, $20\,\mathrm{m\,s^{-1}}$
Frequency of application packets	Every 20 ms
Duration of experiments	30 s for *(04)* and 40 s for *(05)*
Repetitions of experiments	10 repetitions for each parameter combination

Table 3.3: Simulation parameters for the *basic agility experiments* group. Scenarios are generated by combination of all parameters resulting in 648 distinct scenarios.

route selection (see Table 3.3). By using different packet sizes, the links will be utilized at different levels which might affect the agility of a routing protocol due to saturated links. Variable TDMA slot lengths (and along with that different MTU sizes) lead to a difference in latency for the communication over a link which can also affect the agility of the routing protocol. The change in velocity of the several nodes leads to faster or slower changes in topology which can affect the decisions made during route selection. As also seen in the first experiment group, all experiments of the *basic agility experiments* group possess statically configured movement and positioning of the nodes with only a single sender and receiver in each scenario.

By observing the achieved throughput and achieved hop count, insight can be gained on the influence of the packet size and TDMA slot length on the agility of each routing protocol. Additionally, the route establishment latency and packet loss observed in the simulations can be compared between the different routing protocols along with the path each of the routing protocols selected.

3.2.3 Advanced Experiments

Continuing on the focus on more realistic and therefore more complex scenarios, the *advanced experiments* group describes two advanced scenarios which are expected to appear during in-situ space exploration missions. In that context it is mandatory for nodes within a network to transmit packets simultaneously. The experiment *(6)* (see Figure 3.6) depicts three senders and three receivers continuously transmitting data over a three-node full-mesh relay network. The senders are transmitting data to the opposing node on the other side of the network simultaneously (Ⓐ → Ⓗ, Ⓑ → Ⓘ, Ⓒ → Ⓖ). Whilst this experiment features no changes in topology it features a scenario with multiple active transmissions which are usually found in any ad-hoc network. The seventh experiment describes a network fragmenting into two islands of almost the same size. This can happen due to external interference like clouds of dust blocking communication or simply navigation errors. It is mandatory that a routing protocol is still capable of establishing routes even if large parts of the network become unavailable. In this experiment the two islands are continuously diverging from each other in a linear movement until no link exists between the two islands. A sender transmits packets to the receiver throughout the whole simulation and the routing protocol is challenged with huge changes in topology which lead to a multitude of possible

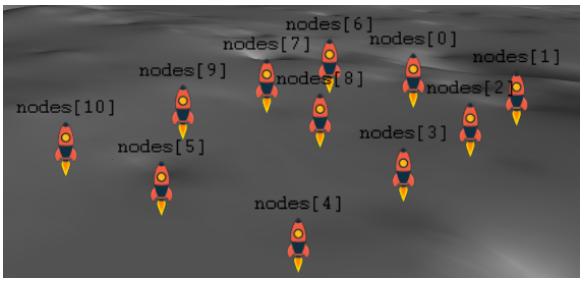

Figure 3.5: The `osgEarth` visualization of experiment *(07)* as seen in the graphical user interface of *Omnet++*.

routes to the destination becoming unavailable. This experiment is also executed in the opposite direction where two islands are joined into a single network where a variety of new and potentially better paths become available.

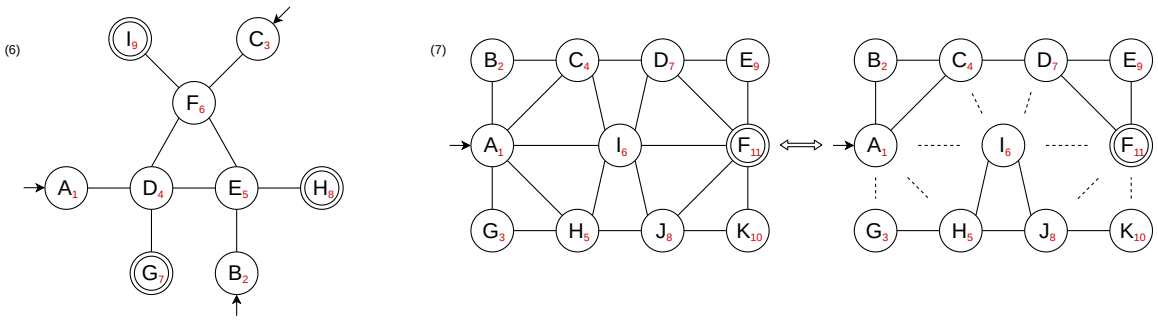

Figure 3.6: The setup of the *advanced experiments* group. The legend for this graph is included in Figure 3.2

For both experiments in the *advanced experiments* group the latency observed during route establishment is especially interesting. The difference to the results from previous experiments will show the impact additional transmissions have on the route establishment. Along with that latency, the packet overhead created by the routing protocol can also differ when compared to the previous experiments. The hop count and packet loss metrics can indicate where a routing protocol failed to meet the optimal route selection. Especially interesting for the larger networks depicted in this experiment group is the total amount of packets processed on each node as it is directly coupled with the energy consumption of the nodes. To prevent early failures of individual nodes in the network an equally distributed energy consumption within the network is preferable.

Parameter	**Values**
Wireless MAC	DLR TDMA MAC, IEEE 802.11 MAC
Deployed routing protocol	DYMO, GPSR, DSDV
Packet size sent from transceiver	$1 \cdot MTU$
TDMA slot length per node	500 µs, 1 ms, 10 ms with 128 B, 256 B, 2048 B MTU
Physical environment	Flat terrain in Boguslawsky crater
Velocity of nodes in *(7)*	$5\,\mathrm{m\,s^{-1}}$, $10\,\mathrm{m\,s^{-1}}$, $20\,\mathrm{m\,s^{-1}}$
Frequency of application packets	Every 20 ms
Duration of experiments	60 s
Repetitions of experiments	10 repetitions for each parameter combination

Table 3.4: Simulation parameters for the *advanced experiments* group. Scenarios are generated by combination of all parameters resulting in 126 distinct scenarios.

The parameterization used in the *advanced experiments* group is described in Table 3.4 and mostly follows the parameterization of the previous experiment groups. The packet size is in contrast to the previous experiments not altered as insights into the routing protocol behavior depending on the packet size are expected to be gained by the previous experiments. Further, the packet size is defined relative to the MTU and will therefore also change along with the MTU in this experiment.

Within the simulation of the *advanced experiments* group, the sent and received packets on the sending and receiving nodes are counted to compare the routing protocol overhead and route establishment latency to the results of the *simple experiments* group. Additionally, the load distribution of processed packets per node can be assessed by counting transmitted packets on all other nodes.

3.2.4 Generated Experiments

The *generated experiments* group complements the previous experiments with a common approach for the evaluation of routing protocols where a group of nodes is applied with a random movement. In addition a worst case scenario is described in experiment *(9)* where nodes are arranged in a chain. The experiments described in the *generated experiments* group consists of scenarios with generated network topology and movement (see Figure 3.7). The experiment template *(8)* simulates a realistic movement of nodes in a swarm. The nodes are initially distributed in a quadratic grid with nodes placed from left to right and top to bottom. A Gauss-Markov mobility controls the movement of each node in the swarm resulting in a highly dynamic topology. By adjusting the swarm size, it can be explored how routing protocols are affected by such dynamic topologies with the amount of nodes participating in the swarm. The experiment template *(9)* focuses specifically on the exploration of the impact of the TDMA based MAC layer on the routing protocols. A chain of nodes is generated with the TDMA indices assigned in opposite direction to the communication direction. The last node of the chain transmits packets to the first node resulting in every node of the network being involved in the forwarding of each packet. By conducting the experiment with differing node count, the stability of connection within such network is tested regarding the length of the chain.

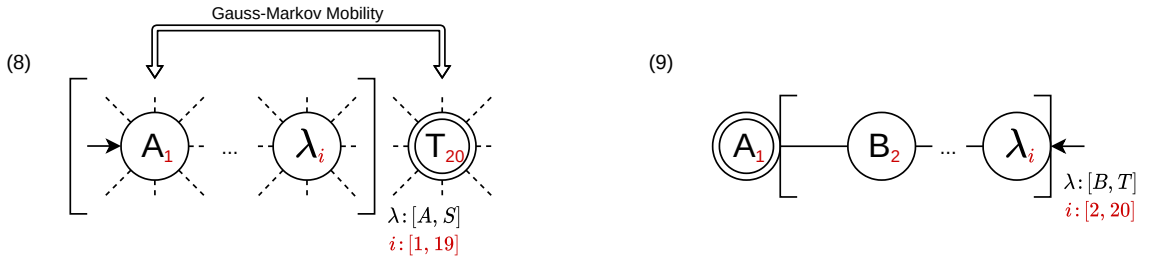

Figure 3.7: The setup of the *generated experiments* group. The legend for this graph is included in Figure 3.2

For both experiment templates the route establishment latency is measured to gain insight on each routing protocol's performance. Additionally, the packet loss experienced during the

experiment runs is measured for comparison of the routing protocols. For the experiment template *(8)* the selected route for each packet is recorded whereas for experiment template *(9)* the overhead produced by the routing protocol for finding a route along the chain of nodes is of more interest. All experiments are run with the IEEE 802.11g MAC as well to identify effects only observable with the TDMA MAC. The full list of parameters utilized in the simulations of the *generated experiments* group is depicted in Table 3.5. As the experiment template *(8)* is featuring a dynamic random movement of nodes, they possess a seeded random number generator which ensures the complete reproducibility of each experiment run.

Parameter	**Values**
Wireless MAC	DLR TDMA MAC, IEEE 802.11 MAC
Deployed routing protocol	DYMO, GPSR, DSDV
Packet size sent from transceiver	$1 \cdot MTU$
Physical environment	Flat terrain in Boguslawsky crater
TDMA slot length per node in *(8)*	500 µs
TDMA slot length per node in *(9)*	500 µs, 1 ms, 10 ms
Velocity of nodes in *(8)*	$5\,\mathrm{m\,s^{-1}}$, $10\,\mathrm{m\,s^{-1}}$, $20\,\mathrm{m\,s^{-1}}$
Frequency of application packets	Every 20 ms
Duration of experiments	30 s
Repetitions of experiments	10 repetitions for each parameter combination

Table 3.5: Simulation parameters for the *generated experiments* group. Scenarios are generated by combination of all parameters resulting in 684 distinct scenarios.

The simulations of the experiment template *(8)* will provide additional insight into the route establishment latencies of the routing protocols, especially when compared to experiment *(1)*. In addition to the length of the selected route of the packets, the overall load distribution within the complete network is observed to gain further insight on the energy consumption of the nodes with respect to the utilized routing protocol. Each routing protocol's overhead observed in *(9)* will be put into perspective to the findings of experiment *(1)*.

3.2.5 Alternative Route Experiments

The *basic agility experiments* group described two experiments with very basic alternative route selection. The *alternative route experiments* group continues on the exploration of handling dynamic topologies with more complex scenarios. This experiment group concentrates on unstable links on the shortest path with the lowest latency. The layouts of the experiments described in this experiment group are taken from Wibling et al. [15] and

slightly altered to model TDMA slot indices. In contrast to previous experiments, both depicted experiments are only describing single experiments. During the simulation run, the experiment continuously transitions between both depicted topologies resulting in very unstable connections.

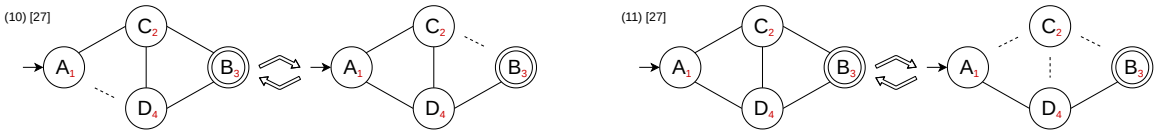

Figure 3.8: The setup of the *alternative route experiments* group. The legend for this graph is included in Figure 3.2

In experiment *(10)* the shortest paths are unstable due to the unstable links Ⓐ — Ⓓ and Ⓒ — Ⓑ. The only stable connection between Ⓐ and Ⓑ is the path over Ⓒ and Ⓓ. However, as Ⓓ has the highest TDMA slot index the latency over that node will be significantly higher. The topology of the experiment is changes every 5 seconds leading to the aforementioned links to appear and disappear every 5 seconds. The experiment *(11)* is very similar to experiment *(4)* however *(11)* enforces the selection of a route as no direct link between sender and receiver exists. In addition the links to Ⓒ are unstable as the topology is changed every 5 seconds between the two depicted state. Depending on the individual mission conducted during in-situ space exploration, the selection of stable paths in favor of short-latency or low hop count might be preferable while low latencies might be favored during other missions. Nevertheless, the behavior observed during the simulation of this experiment group is of great interest when selecting a routing protocol for such a mission.

Parameter	**Values**
Wireless MAC	DLR TDMA MAC, IEEE 802.11 MAC
Deployed routing protocol	DYMO, GPSR, DSDV
Packet size sent from transceiver	$1 \cdot MTU$
TDMA slot length per node	500 µs, 1 ms, 10 ms with 128 B, 256 B, 2048 B MTU
Physical environment	Flat terrain in Boguslawsky crater
Velocity of nodes	$10\,\mathrm{m\,s^{-1}}$
Frequency of application packets	Every 20 ms
Duration of experiments	60 s
Repetitions of experiments	10 repetitions for each parameter combination

Table 3.6: Simulation parameters for the *alternative route experiments* group. Scenarios are generated by combination of all parameters resulting in 36 distinct scenarios.

The experiments of the *alternative routes experiments* group are similarly parameterized as previous experiment groups although focusing on the variation of the TDMA slot length (see Table 3.6). The experiments are expected to show differences in the routing protocols behavior when changing the TDMA slot length as the latency for routes over Ⓓ will change with the TDMA slot length. For measuring the hop count, packet loss, route establishment latency, and routing protocol overhead, the sent and received packet on each node will be collected and the chosen route for each packet. The experiments are expected to gain insight into the created routing protocol overhead if unstable links are present by comparing the results to previous simulation runs from the *simple experiments* group. Furthermore, the tendency of a routing protocol to prefer stable connections in favor of short or low latency ones can be observed. The route establishment latency might differ in a network with very unstable links as routes over that links might fail during route establishment. By comparing the results to previous experiments, an assessment can be made on the ability of a routing protocol to recognize such unstable links and choosing alternative routes.

CHAPTER 4

Thesis Outcome

4.1 Evaluation

This section is organized in two parts. In the first part, the behavior of the routing protocols is compared regarding operation on the TDMA MAC and on the IEEE 802.11g MAC. The second part focuses on the differences in behavior and performance of the individual routing protocols, including the agility of the protocols to react to topology changes, route selection strategies, and the estimated energy consumption of the nodes within a network.

4.1.1 Influence of the TDMA MAC on the Performance of the Routing Protocols

All experiments conducted in the context of this work were executed on the TDMA MAC as well as on the standard IEEE 802.11g MAC. As a result, the performance of each routing protocol can be compared on both MACs for each of the conducted experiments. This allows the observation of differences introduced by the TDMA scheme of the DLR MAC and helps to estimate the requirements for routing protocols and applications running on that MAC. Several different metrics were recorded during the simulation of the experiments where the findings from the *simple experiments* group reveal the first major differences found during the operation of the different routing protocols regarding the MACs.

The throughput measured during the first experiment of the *simple experiments* group is depicted in Figure 4.1 and consists of the average throughput observed at a given point in time throughout all experiment runs (including repetitions of runs with the same configuration). The figure visualizes the throughput regarding the utilized MAC and MTU where the MTU is coupled to a specific TDMA slot length on the TDMA MAC by experiment design as previously described in Section 3.2. The observation shows that the throughput rises with an increase of the MTU. This is due to the packet size of the application packets being relative to the MTU and therefore yielding larger packets for higher MTU configurations. The packets produced by the UDP application on the transceiving node are sent in regular intervals of 20 ms regardless of other parameters, therefore the increase in MTU will naturally lead to a higher throughput. This effect can be observed similarly on

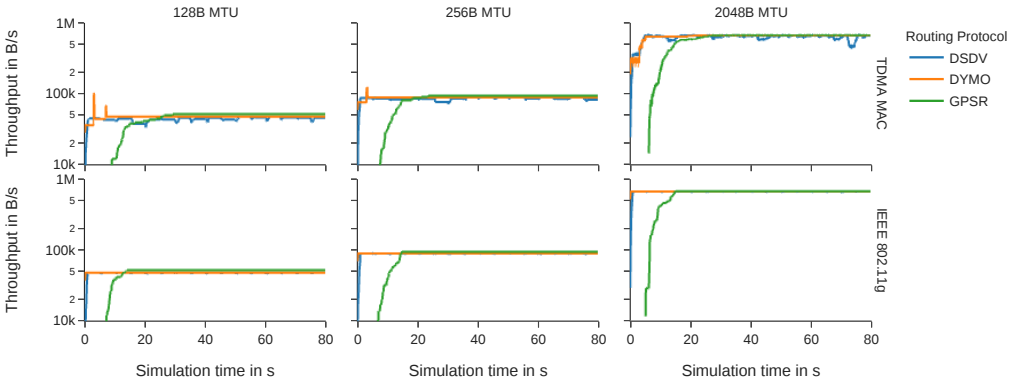

Figure 4.1: Application data throughput on receiving node regarding several MTU configurations over time in experiment *(01)* comparing the utilized MACs and routing protocols

both MACs. However, the visualization of the throughput observed on the TDMA MAC reveals a more unstable operation the IEEE 802.11g MAC. This effect is neither created by the UDP application nor the routing protocols respecting the TDMA cycles of the TDMA MAC. Packets have to wait for varying durations after their arrival in the MAC layer for the transmission to begin. As opposed to the TDMA MAC, the IEEE 802.11g MAC has almost uninterrupted channel access within the simulation scenario where application packets are transmitted as soon as they are available in the MAC layer. Similar observations can be made in all of the other experiments.

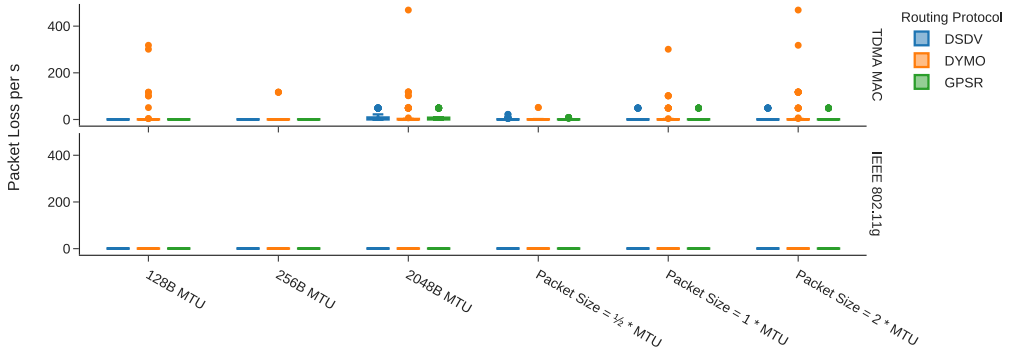

Figure 4.2: Number of packets lost per second in experiment *(01)* comparing the utilized MACs and routing protocols

Apart from the throughput, the number of packets which were transmitted by the MAC on the transceiving node were compared against the received packets on the destination node. This allows for the computation of a packet loss which differs from normal application packet

loss as only the packets transmitted by the MAC are being reflected in the metric. This reveals the specific packet loss introduced by the utilized routing protocol, instead of packet losses induced by experiment design (e.g. impossible connections due to the node being out of communication range) or other protocol layers such as UDP. The packet loss observed in all experiments shows that generally slightly more packets are lost on the TDMA MAC than on the IEEE 802.11g MAC. This is especially visible in the first experiment as depicted in Figure 4.2. The graph visualizes how the packet loss changes with different configurations where each simulation run is represented by the minimum, maximum, and average packet loss per second. The visualization reveals that the packet loss on the TDMA MAC is higher for individual simulation runs than the packet loss seen on the IEEE 802.11g MAC especially for simulations configured with higher MTU. Although the majority of simulation runs on the TDMA MAC show the same behavior as the IEEE 802.11g MAC, the operation on the TDMA MAC is less stable. The increased packet loss is likely created by the additional time necessary for routing protocols to exchange or gain routing information on the TDMA MAC. Packets sent by the routing protocols must wait on the node until the TDMA cycle allows a transmission on the channel. This waiting time can be incorporated into the operation of the routing protocols and the observed effect eliminated by making the protocols and applications aware of the TDMA cycle. In summary, the throughput and packet loss show a less stable operation of the TDMA MAC in the *simple experiment* group, which is confirmed by observations in other experiment groups.

Observation 1 *Although it is possible to run protocols and applications which are unaware of the TDMA cycle on the TDMA MAC, instability in operation of that applications can be observed on the TDMA MAC when compared to the performance of the same applications on an IEEE 802.11g MAC.*

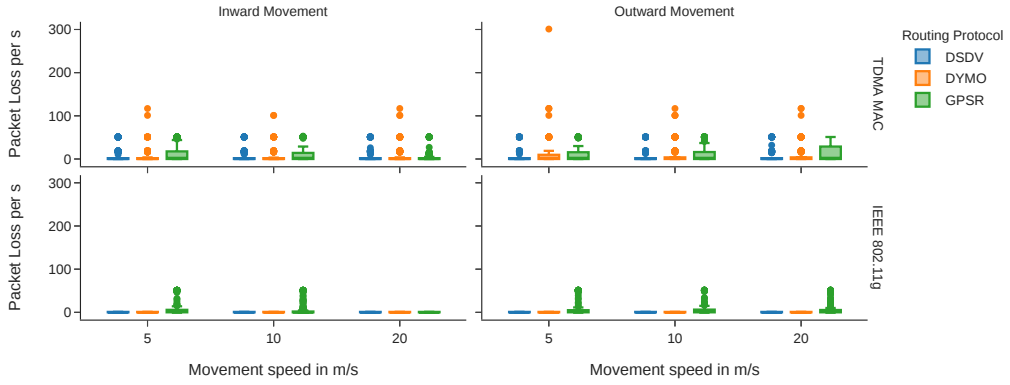

Figure 4.3: Number of packets lost per second in experiment *(04)* comparing the utilized MACs and routing protocols

The influence of the TDMA MAC on the packet loss becomes more prevalent in experiment *(04)* of the *basic agility experiments* group as seen in Figure 4.3. The experienced packet loss on the TDMA MAC increases for all routing protocols. The design of this experiment

incorporates a third node into the simulation which implements movement in two different variants of the experiment as described in Section 3.2.2. As the route selection analysis in Section 4.1.3 will reveal, none of the routing protocols utilized the third node for an alternative route to the destination node. Nonetheless, the packet loss increased when compared to experiment *(01)*. As this increase in packet loss is not seen on the IEEE 802.11g MAC, it is likely created by the longer TDMA cycle created by the third node in the network. It is important to bear in mind that the TDMA cycle length does not change when the third node leaves the communication range of the other two nodes. The TDMA configuration is completely static over the whole duration of the simulation. Further, the packet loss experienced during simulation runs utilizing the GPSR routing protocol show an increased packet loss even on the IEEE 802.11g MAC.

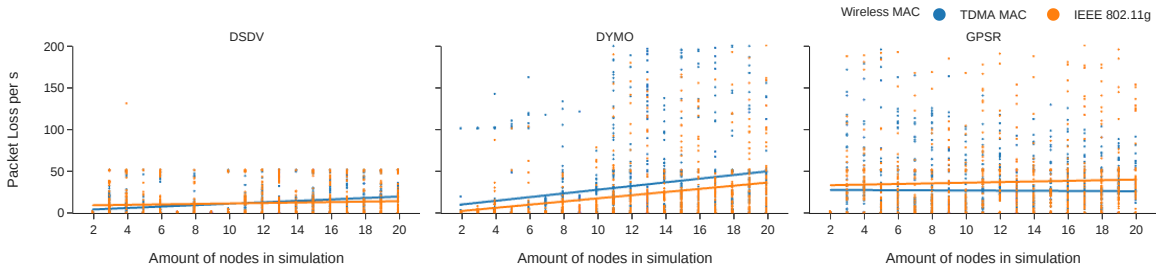

Figure 4.4: Number of packets lost per second in experiment *(08)* comparing the utilized MACs and routing protocols

Experiment *(08)* of the *generated experiments* group reveals the development of the packet loss with an increasing network size. Figure 4.4 visualizes the development of packet loss with network size for the routing protocols on both MACs. Generally, the increase in packet loss on the TDMA MAC is higher than on the IEEE 802.11g MAC. The decrease in packet loss for the GPSR protocol seen on the TDMA MAC is caused by the protocol not establishing a connection at all, resulting in no packets being transmitted by the TDMA MAC in the first place and therefore leading to a decline in packet loss observed under this metric.

Observation 2 *Longer TDMA cycles and along with that an increasing network size further increase the instability of applications and protocols unaware of the TDMA scheme running in a network node driven by the TDMA MAC.*

Further investigation of the more complex experiments reveals additional differences between the two MACs. Experiment *(06)* of the *advanced experiments* group focuses on the simultaneous transmission of application packets from three transceivers to three different receivers. All nodes within the network of that experiment generate the same amount of application packets of the same size and in the same frequency. By looking at the throughput achieved on the nodes, as depicted in Figure 4.5, it can be seen that the throughput achieved on the TDMA MAC is higher on the node with the lowest TDMA slot index (node Ⓖ). Additionally, the throughput observed on the TDMA MAC is roughly one half of the throughput seen on the IEEE 802.11g MAC.

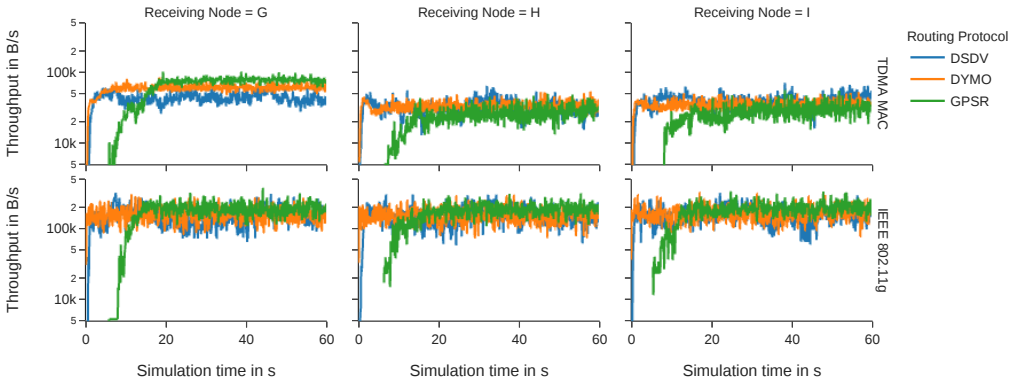

Figure 4.5: Application data throughput as observed on each receiving node over time in experiment *(06)* comparing the utilized MACs and routing protocols

Observation 3 *The utilization of three transceivers within a network of nine nodes utilizing the TDMA MAC achieves less throughput than a network utilizing the IEEE 802.11g MACs in the same setup. Further, the node with the lowest TDMA slot index achieves more throughput than the other transceivers in the network.*

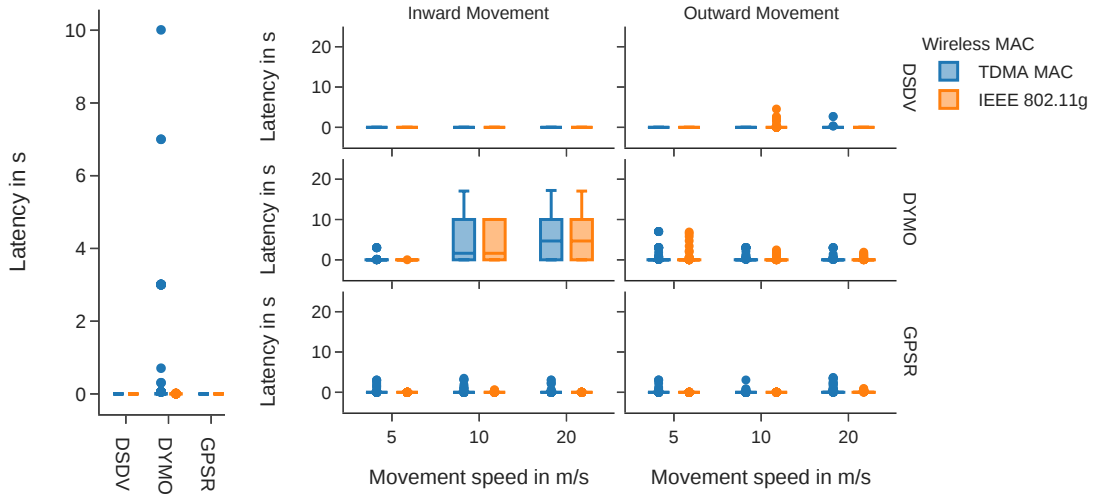

a) Experiment *(01)* b) Experiment *(05)*

Figure 4.6: Measured route establishment latency in experiment *(01)* and *(05)*

Continuing with the analysis of effects introduced by the TDMA MAC, the establishment of routes in the *simple experiments* group reveals very low latencies for the majority of simulation runs on both MACs whereas the TDMA MAC experiences higher latencies in a minority of simulations utilizing the DYMO routing protocol, see Figure 4.6a. Whilst a movement of nodes in the *simple experiments* group with networks containing only two

nodes results in little difference between the utilized MACs, the introduction of more complex network layouts which possess more than two nodes shows a slightly higher route establishment latency on the TDMA MAC, especially for the GPSR routing protocol as seen in Figure 4.6b.

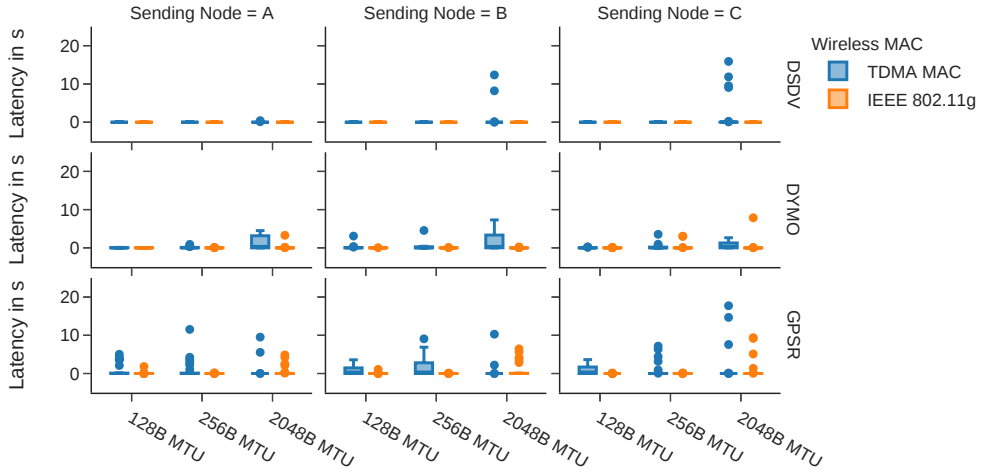

Figure 4.7: Measured route establishment latency for each routing protocol on both utilized MACs in experiment *(06)*

Examining experiments which not only contain more nodes, but also feature multiple simultaneously transceiving nodes as implemented in experiment *(06)* of the *advanced experiments* group, reveals an increasing route establishment latency along with a rising MTU configuration as seen in Figure 4.7. This is observed on both MACs while being more prominent on the TDMA MAC. This confirms the observations on the packet loss where more complex networks yield to slightly more unstable operation under the TDMA MAC with the slower route establishment observed in such networks.

4.1.2 Agility of the Routing Protocols

Apart from analyzing the influences of the TDMA scheme on a networks operation, this work also examines the operation of three different routing protocols within the experiment's networks. This section will focus on the agility of the routing protocols and will discuss the observations of the TDMA scheme of DLR's MAC in detail.

The *simple experiments* group depicts the most simple network layouts. This simplicity allows gaining insight into the basic characteristics of each routing protocol. The routing protocol overhead depicted in Figure 4.8 for experiment *(01)* describes the amount of routing protocol data transmitted per second in relation to the amount of application data transmitted in that time frame. The metric reveals small regular peaks in routing protocol overhead for the proactively operating DSDV routing protocol induced by additional

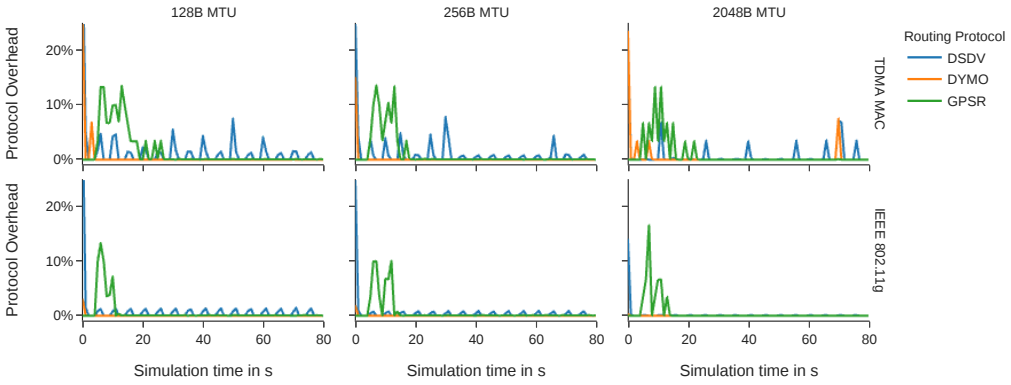

Figure 4.8: Measured routing protocol overhead relative to all transmitted application packets regarding several MTU configurations over time in experiment *(01)*

packets transmitted for route discovery. As a reactive routing protocol, DYMO shows a peak at the very start of the simulation with very low overhead throughout the rest of the simulation. Remarkably, the GPSR protocol shows a higher and longer overhead at the beginning of the simulation created by the beaconing needed to distribute positioning information to neighboring nodes. Later in the simulation, the overhead decreases as the positioning information is attached to the MAC headers of each transmitted application packet. When observing the achieved throughput of the GPSR protocol within the same simulation, the GPSR routing protocol shows a slow start in all configurations where the target throughput is only reached after 15 to 20 seconds in the simulation, see Figure 4.1. This is due to the node Ⓐ in experiment *(01)* not knowing of the existence of node Ⓑ as Ⓑ has not sent a beacon containing positioning and therefore routing information, yet. Only after Ⓑ has transmitted the first beacon, Ⓐ will start the transmission of application packets. Further note, that the throughput observed for the GPSR protocol is slightly higher after successful route establishment due to the additional data placed by the routing protocol in the application packets containing the positioning information of the previous node.

Observation 4 *The main characteristics of all the routing protocols are observable in the simulations and apart from the previously discussed instability of applications and routing protocols on the TDMA MAC, match the observations made on the IEEE 802.11g MAC.*

Expanding the analysis to more complex experiment setups which introduce movement to the networks as featured in experiment *(02)* and visualized in Figure 4.9, less frequent peaks of routing protocol overhead can be observed for the DYMO protocol when no connection is established and impossible by experiment design. Similar observations were made during all experiments where a connection loss due to experiment design occurs.

A look at the achieved throughput of the experiment in Figure 4.10 reveals the influence of movement on the routing protocols. The first variant of the experiment *(02)* involves

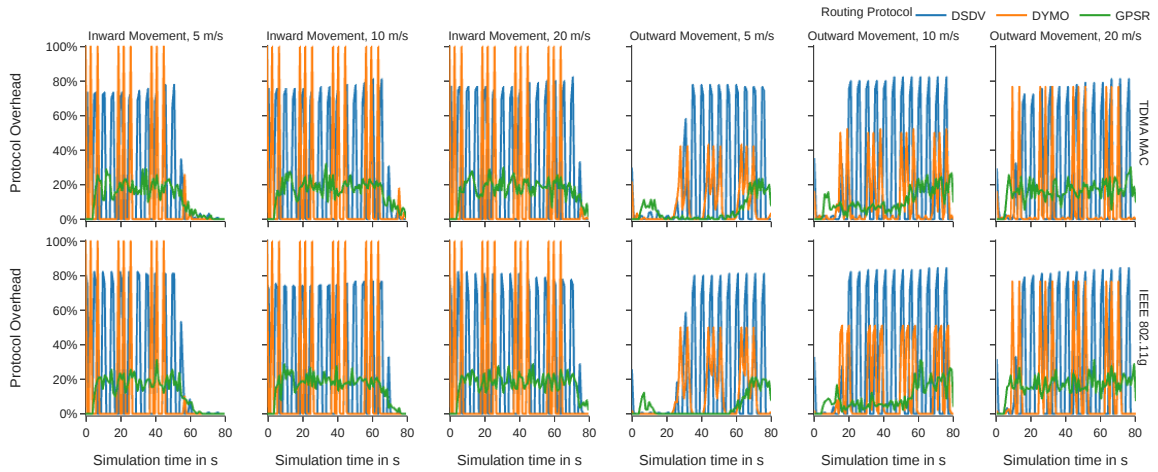

Figure 4.9: Measured routing protocol overhead relative to all transmitted application packets regarding speed and direction over time in experiment *(02)*

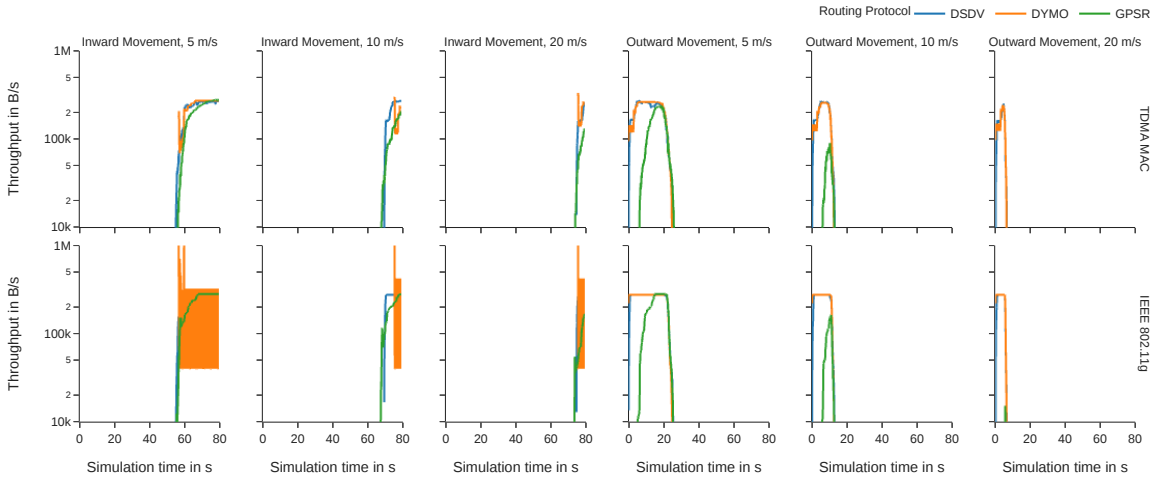

Figure 4.10: Application data throughput on receiving node regarding speed and movement direction over time in experiment *(02)* comparing the utilized MACs and routing protocols

an inward movement with a connection establishment later in the simulation. All routing protocols react equally fast to the establishment of the new connection. In contrast to previous experiments, the IEEE 802.11g MAC shows rapid jumps in the achieved throughput, performing worse than the TDMA MAC. Notably, the GPSR protocol performs better during the inward movement when compared to experiment *(01)*. Additionally, the same delay observed in *(01)* is visible in the second variant of this experiment where Ⓑ moves outward resulting in a connection loss between the two nodes later in the simulation. This indicates that the GPSR protocol requires a warmup time where each node needs to transmit a beacon to the other nodes first, and thereby providing the minimal required routing information. When additionally comparing the connection establishment during inward

movement with the routing protocol overhead shown in Figure 4.9 a fast reaction to the change in topology by GPSR and DSDV is observed. The DYMO routing protocol, however, is slower in realizing the topology change whereas GPSR shows the fastest reaction regardless of the movement speed.

Observation 5 *Proactive and greedy routing approaches yield better agility when compared to reactive routing due to less frequent route discovery.*

Apart from the routing protocol overhead, Figure 4.2 visualizes the observed packet loss on the TDMA and IEEE 802.11g MAC. The previously discussed increased packet loss on the TDMA MAC is especially problematic for the DYMO routing protocol which experiences more packet loss than all the other routing protocols regardless of the configuration. This is further supported by the observations seen in Figure 4.6a where the minimum, maximum, and average route establishment latency for each simulation run is visualized regarding the same experiment parameters. For individual simulation runs the reactive routing approach of the DYMO routing protocol results in higher packet loss and route establishment latencies. Due to the greedy nature of the GPSR routing protocol and the proactive approach of DSDV, there is only a very small route establishment latency observable.

Observation 6 *Utilizing a reactive routing approach on the TDMA MAC is sightly inferior to proactive or greedy approaches regarding the reaction time of the protocol.*

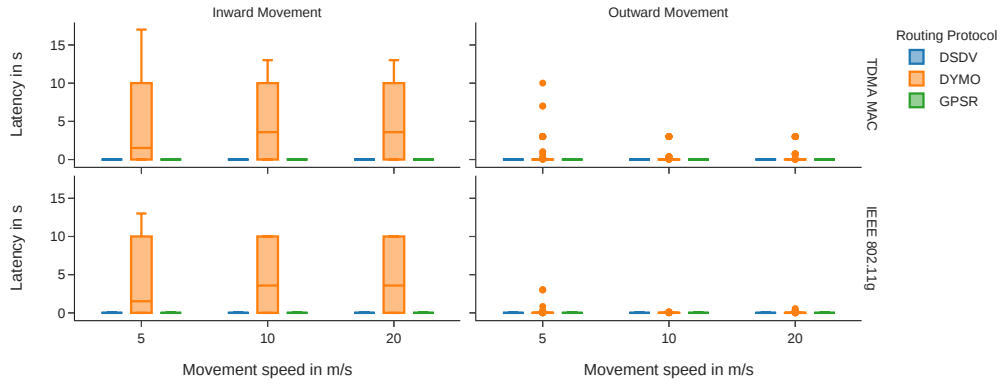

Figure 4.11: Measured route establishment latency for each routing protocol on both utilized MACs in experiment *(02)*

In Figure 4.11 the route establishment latency is depicted for the experiment *(02)* of the *simple experiments* group. Due to the frequent proactive route updates performed by DSDV and the greedy nature of GPSR the route establishment latency is low even under fast movement. The inferior capability of DYMO to react to topology changes due to less frequent updates leads to a moderate route establishment latency. The inward movement of the receiving node in experiment *(02)* yields to the establishment of a new connection mid-simulation. During the outward movement a connection can be established from the

very start of the simulation as all the nodes are within communication range. However, during inward movement the dynamic establishment of a connection later in the simulation leads to worse route establishment performance. This confirms the previous observation that DYMO is less agile in handling topology changes. The observation is further confirmed by similar observations in Figure A.2 of experiment *(05)* and Figure A.3 of *(07)*.

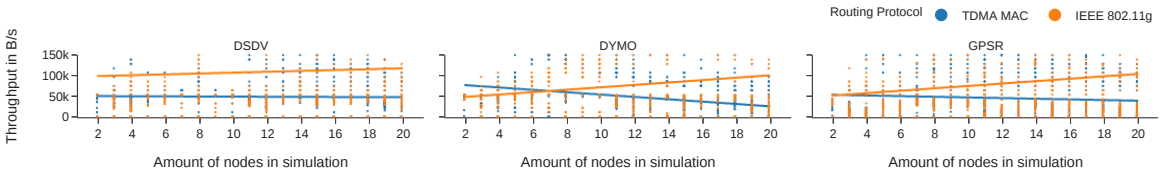

a) Application data throughput on receiving node

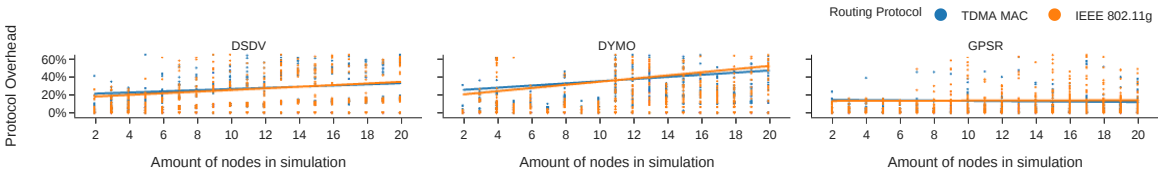

b) Measured routing protocol overhead

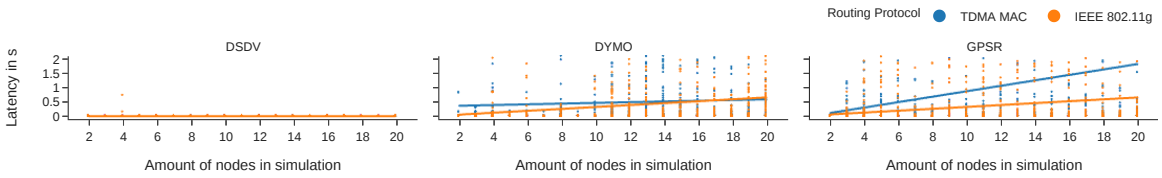

c) Measured route establishment latency

Figure 4.12: Measurements for the experiment *(08)* of the *generated experiments* group

The *generated experiments* group concentrates on the deployment of varying network sizes in order to gain insight into potential problems created by larger network sizes. The experiment *(08)* implements a traditional approach where nodes are moving randomly within an area where a single sender transmits application packets to a single destination. Whereas the DSDV routing protocol handles an increasing network size very well with a constant route establishment latency as seen in Figure 4.12c, DYMO shows an increase in route establishment latency with rising network sizes. This increase is stronger in the IEEE 802.11g MAC and occurs stronger on networks with sizes greater than 10 nodes. Furthermore, an increase in network size results in a decrease in throughput as visualized in Figure 4.12a with all routing protocols and on all MACs whereas the routing protocol overhead is increasing with the network size with all routing protocols except for GPSR.

Observation 7 *The agility of the proactive DSDV routing protocol does not decline with an increasing network size but the reactive DYMO and greedy GPSR protocols perform worse with an increasing network size.*

Continuing on the examination of the influence of rising network sizes, experiment *(09)* has been designed to specifically gain insight into the effect of the TDMA scheme on the

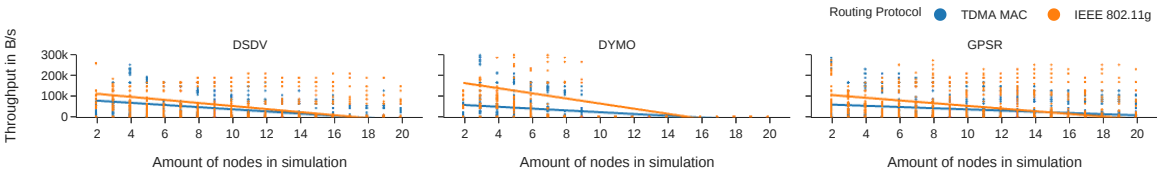

a) Application data throughput on receiving node

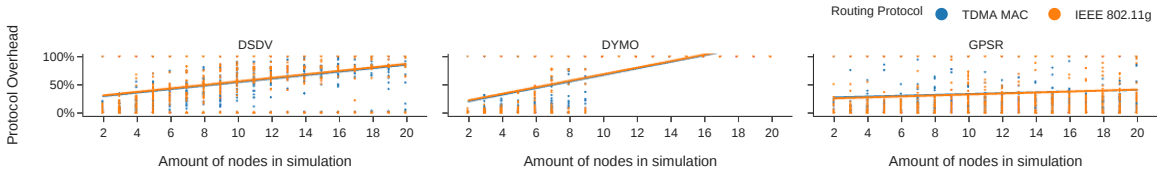

b) Measured routing protocol overhead

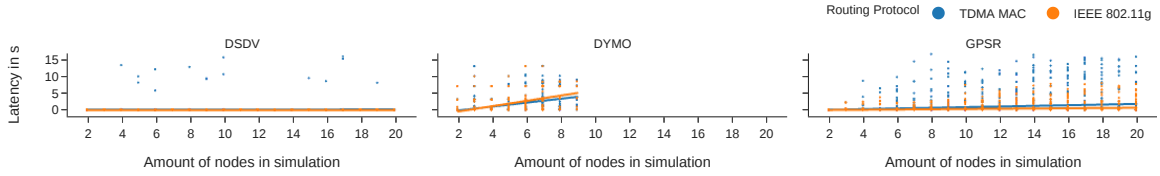

c) Measured route establishment latency

Figure 4.13: Measurements for the experiment *(09)* of the *generated experiments* group

performance of the routing protocols. The networks generated in this experiment consist of a chain of nodes as described in Section 3.2.4. Figure 4.13c visualizes the observed route establishment latency with a rising network size and therefore a longer chain of nodes needed to establish a connection between sender and receiver. However, no severe impact of the TDMA scheme on the performance of the routing protocols can be observed when compared to the performance of the routing protocols with an IEEE 802.11g MAC. The visualization of the throughput observed within experiment *(09)* further reveals that the performance of all the routing protocols degrades with longer hop chains regardless of the utilized MAC. The DYMO routing protocol prevents the establishment of a route with 10 or more hops in its default configuration and is therefore not able to establish routes with networks sizes of 10 nodes or more within this simulation setup.

Observation 8 *The TDMA channel access has no severe impact on the performance of any of the routing protocols when compared to the results of the IEEE 802.11g MAC. Except for the observations previously made in other experiments, the TDMA MAC does not introduce any other observable disadvantages.*

4.1.3 Route Selection

The performance of a routing protocol largely depends on the routing decisions issued by the protocol. The selected route has many influences on a network such as the distribution of energy consumption in the network, the time it takes for a packet to reach its destination, or the stability of a connection. This section will analyze the data collected during the simulation runs with different metrics to gain insight into the route selection strategies of

the protocols.

Starting with a look at the routing protocol overhead in Figure 4.9 of experiment *(02)*, fundamental differences between the routing protocols are revealed. The GPSR routing protocol shows a continuous routing protocol overhead when no connection is physically possible. This effect is created by the greedy routing approach of GPSR where packets search their route through the network. This is in contrast to DSDV and DYMO where the measured overhead created by the routing protocol is significantly higher when no physical connection between the nodes is possible due to no application packets being transmitted in the network and therefore the routing packets being the only data being transmitted in the network. While DSDV is checking for new routes in regular intervals, DYMO is only checking for new routes every 10 s in its default configuration which leads to the inferior agility when compared to the other routing protocols.

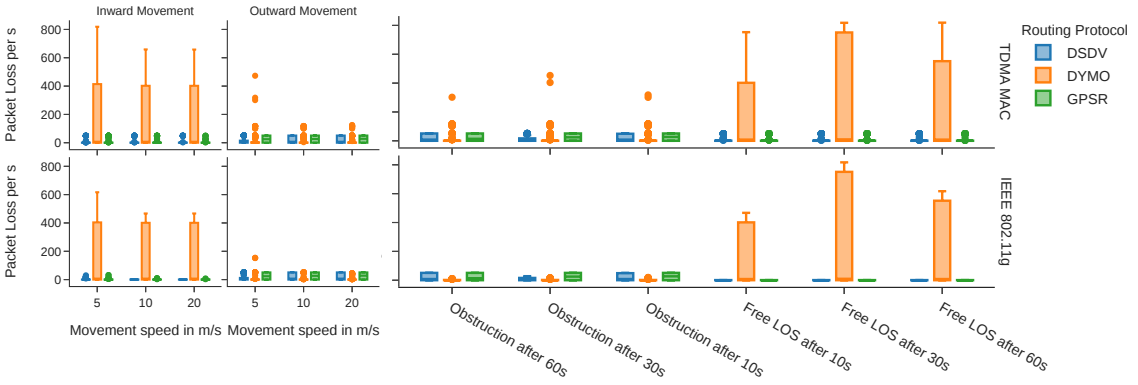

a) Experiment *(02)*

b) Experiment *(03)*

Figure 4.14: Comparison of the number of packets lost in experiment *(02)* and *(03)*

In contrast to the observations in experiment *(02)*, a connection establishment later in the simulation as depicted in the free line-of-sight scenarios in experiment *(03)* visualized in Figure 4.14b and inward movement in experiment *(02)* visualized in Figure 4.14a, the GPSR protocol experiences considerably less packet loss. This is due to the node having no knowledge about its neighbors until the point where the first connection is possible and thus is incapable of starting a greedy or perimeter search for the destination node. The DYMO and DSDV routing protocols however, send packets to the destination node only if a route is known at the moment of departure from the source node. This results in little packets lost en route but instead being held back for transmission by the routing protocol on the source node.

Observation 9 *The behavior of GPSR depends on the previous knowledge a node has gained on its surroundings. This is usually only the case at the very beginning of a nodes operation or when the routing state on a node is cleared.*

Observation 10 *The greedy approach of GPSR cannot prevent the transmission of application packets on the source node if no route to the destination node physically exists but*

the source node has neighboring nodes.

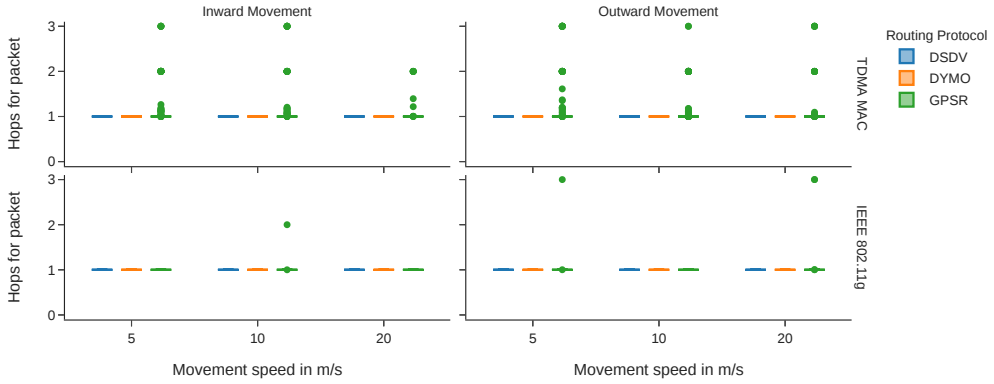

Figure 4.15: The number of hops visited by a received packet on the destination node in experiment *(04)*

As the experiment *(04)* features the possibility to utilize a non-direct connection to the destination node, the number of hops a packet visited when arriving at the destination node can hint whether the third node was visited during the packets traversal through the network. The number of hops is visualized in Figure 4.15 where for each simulation run the minimum, maximum, and mean hop count for each received packet on the destination node is shown regarding the utilized MAC and movement. On both, the TDMA MAC and the IEEE 802.11g MAC the DYMO and DSDV routing protocols chose the direct path to the destination node. However, GPSR features simulation runs where the hop count of packets even reached 3, meaning that the packet must have visited one node twice and therefore routed in a loop. This effect is worse on the TDMA MAC.

Observation 11 *The GPSR routing protocol routed in a loop on both MACs although the effect is more severe on the TDMA MAC.*

The movement speed of the third node within the experiment *(04)* has little influence on the behavior of the routing protocols. GPSR is an exception to this where the protocol performs better during a rapid inward movement of the third node on the TDMA MAC. A rapid inward movement means that the third node is outside the communication range of the other nodes most of the time in the simulation. The third node approaches the two other nodes with high velocity from far away and only enters communication range at the very end of the simulation. The better performance of GPSR is thought to be a result of the missing knowledge on the third node within the network. The lack of knowledge of that node prevents GPSR from including the node in its greedy routing approach. This observation is further supported by the packet loss and route establishment metrics for that experiment as visualized in Figure 4.3 and 4.16.

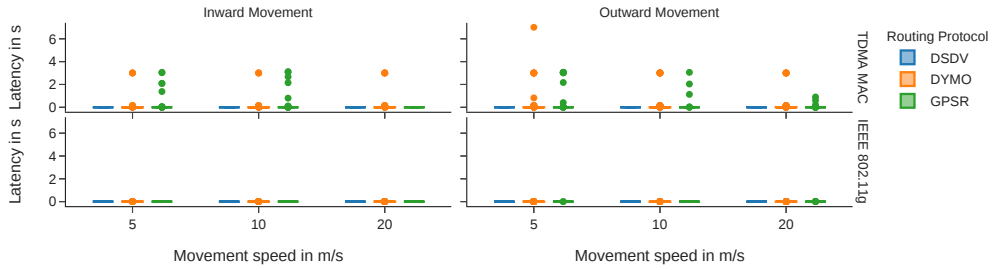

Figure 4.16: Measured route establishment latency for each routing protocol on both utilized MACs in experiment *(04)*

Observation 12 *The existence of a node not necessary for a successful connection has influence on the performance of the GPSR protocol but not on the DSDV and DYMO routing protocols.*

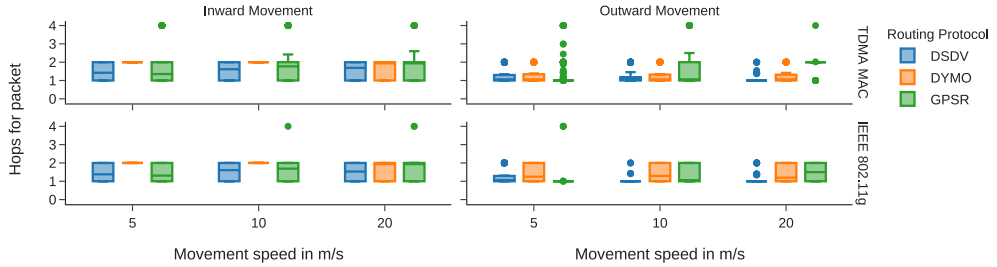

Figure 4.17: The number of hops visited by a received packet on the destination node in experiment *(05)*

Experiment *(05)* from the *basic agility experiments* group is designed to make a third node necessary for the establishment of a successful connection. The node must be established as a relay when the source and destination nodes get out of direct communication range. During inward movement no connection is initially possible. Later in the simulation, the source and destination node enter the communication range of the relay node. The inward movement continues until a direct connection between the source and destination node is possible. All routing protocols except the DYMO routing protocol first start with the long route over the relay node and later transition to the direct route as seen in Figure 4.17. DYMO stays on the long route and does not recognize the emerging direct connection to the destination. During outward movement the source and destination node start within communication range and move away from each other leading to a reversed scenario as depicted in the first variant. All routing protocols initially chose the short path and are later forced to switch to the longer path over the relay node. During slow outward movement the GPSR protocol is incapable of establishing the longer route over the relay node, resulting in the throughput degrading earlier than observed for the other protocols, see Figure A.1.

Observation 13 *DYMO is less agile when compared to DSDV and will not choose a shorter route if another route is already established. A path will only be changed if the connectivity over an established path vanishes.*

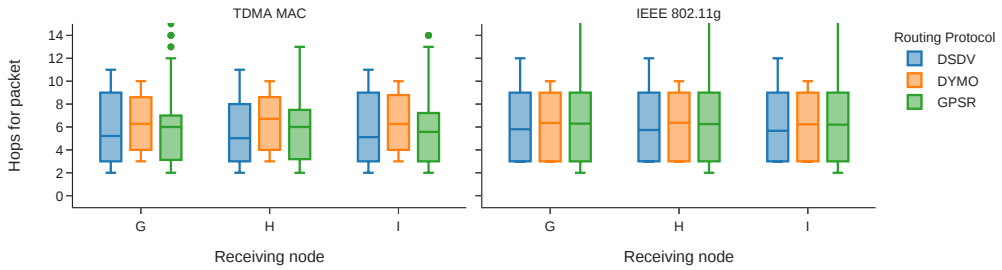

Figure 4.18: The number of hops visited by a received packet on the destination node in experiment *(06)*

In a setup with multiple transceiving nodes as depicted in experiment *(06)* of the *advanced experiments* group, it is apparent that none of the routing protocols were able to establish the shortest path to its destination node. All routing protocols chose routes involving 5 hops or more on average, whereas the shortest route would take 3 hops. Unfortunately, a minority of simulation runs allowed the utilization of a route including only 2 hops indicating a flaw in experiment design where a transceiving node is capable of omitting its direct neighbor in the relay triangle of the network. This indicates that the distance between the nodes in the network was not properly chosen to prevent unplanned connections within the communication range of the nodes.

Observation 14 *All routing protocols are incapable of selecting the shortest route to the destination on both MACs within a scenario where multiple nodes are establishing connections simultaneously.*

The experiment *(07)* implements a network fragmentation where a subnet departs from the rest of the network and in a second variant joins the network through movement. The transceiving node sends packets to a destination node on the other side of the network where the shortest path involves both fragments of the network. During the inward movement of the separated subnet DYMO is the only protocol not selecting the shorter path as soon as it gets available as visualized in Figure 4.19 and thereby confirming observations of DYMO's tendency to not depart from working routes. DSDV and GPSR are both capable of recognizing the shorter route and transition to it accordingly. Notably, this experiment confirms the observation of GPSR occasionally routing in long paths which contain loops. Due to the high node count, the throughput achieved with the IEEE 802.11g MAC is significantly higher than the throughput measured on the TDMA MAC.

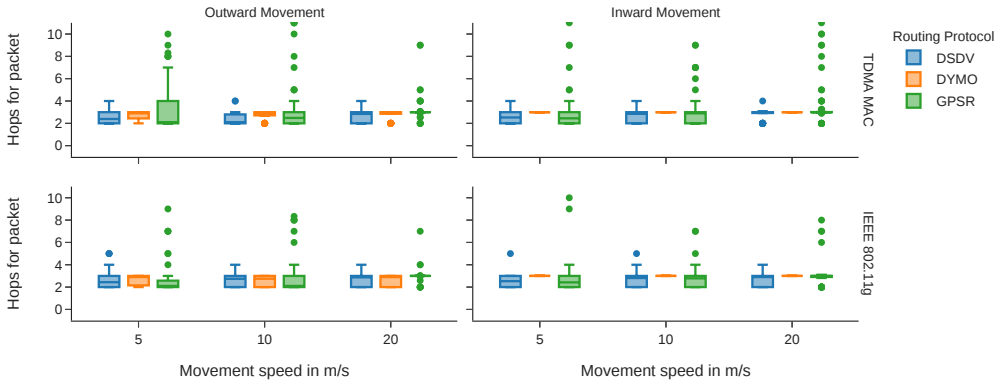

Figure 4.19: The number of hops visited by a received packet on the destination node in experiment *(07)*

Observation 15 *The routing decisions of all routing protocols are consistent with the observations made in the previous experiments, even though this experiment features substantially more nodes within the network.*

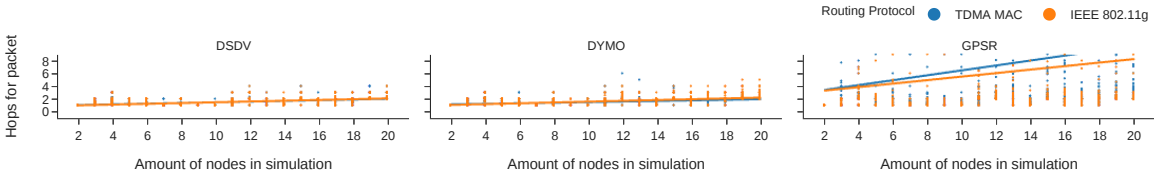

Figure 4.20: The number of hops visited by a received packet on the destination node in experiment *(08)*

In order to assess how the routing protocol's behavior changes with an increasing network size, the experiment *(08)* of the *generated experiments* group has been designed to depict a realistic movement of nodes within a constrained area where a single communication pair establishes a connection and transmits application data. The experiment is conducted with network sizes ranging from 2 nodes up to 20 nodes. Due to the random movement in the network, the general amount of hops needed to establish the connection is low despite large networks. The observation of the number of hops required for a packet to reach its destination is similar between the DSDV and DYMO routing protocols and does not adjust with a change in network size, see Figure 4.20. However, the GPSR routing protocol struggles to establish routes in larger networks and tends to yield very long routes.

Observation 16 *The DSDV and DYMO routing protocols are capable of handling larger network sizes whereas GPSR performs poor on larger networks regardless of speed or utilized MAC.*

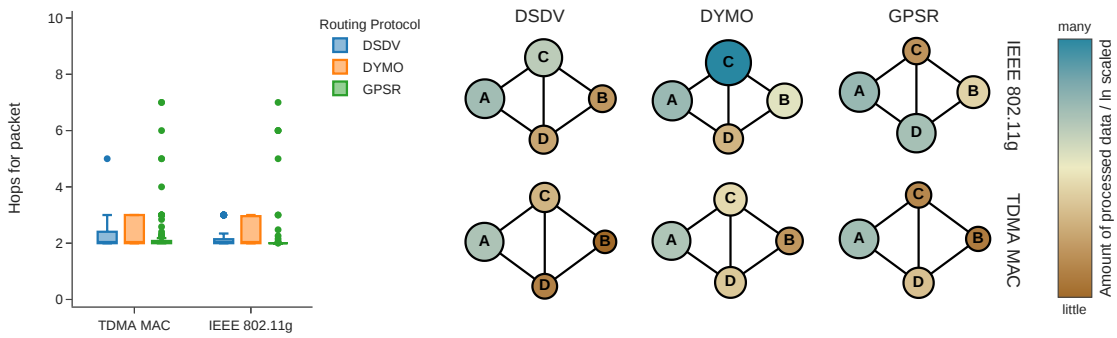

a) Visited hops for received packets

b) Processed data volume for each node

Figure 4.21: Measurements recorded at the experiment *(10)* of the *generated experiments* group visualizing route selection

In contrast to the previously conducted experiments, the *alternative route experiments* group implements experiments with a regularly changing topology. The experiment *(10)* of that group resembles a continuously changing network topology where the longest path in the network is the only stable path to the destination. In Figure 4.21b the aggregated average amount of processed incoming and outgoing data for each of the nodes within the network of the experiment is visualized. As the incoming and outgoing data is aggregated, all relay nodes show twice the processed data when compared to the source and destination nodes. In the event of frequent packet losses, the measured data processed on the source and destination node differs. As none of the routing protocols on either MAC show equal amounts of data processed on the nodes Ⓒ and Ⓓ and additionally not featuring an average hop count of 3, none of the routing protocols chose the long but stable path over Ⓒ and Ⓓ permanently. However, DYMO is using this path sporadically but switching back to the shorter path over Ⓒ as seen in Figure 4.21a.

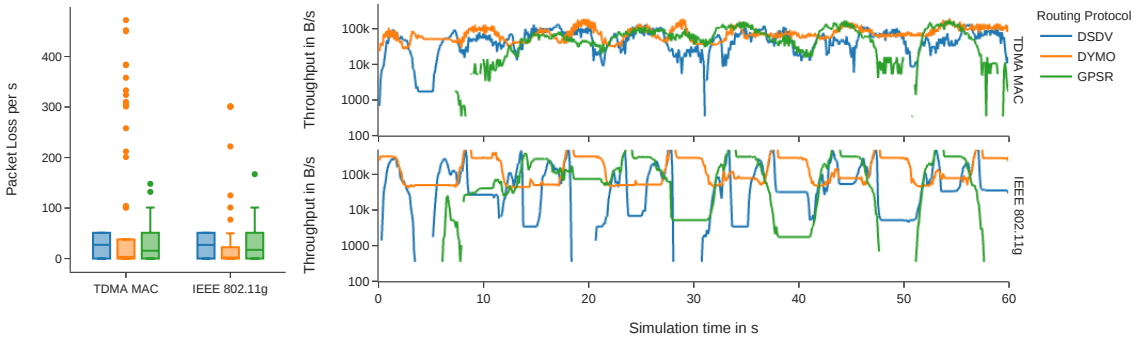

a) Number of packets lost per second

b) Application data throughput on receiving node

Figure 4.22: Measurements recorded at the experiment *(10)* of the *generated experiments* group regarding performance characteristics

Although none of the tested routing protocols chose the stable path permanently for the establishment of a connection to the destination node, DYMO is able to maintain a continuous throughput on both MACs as visualized in Figure 4.22b. Notably, the observed throughput is more stable on the TDMA MAC. DSDV and GPSR feature a lower throughput which occasionally stalls, which is especially visible on the IEEE 802.11g MAC featuring not only less throughput but also complete connection losses where the protocols are able to ensure connectivity on the TDMA MAC. The packet loss observed, depicted in Figure 4.22a, confirms breaking connections which are not reestablished quick enough to prevent stalling and with that packet loss. These observations are in contrast to results from the previous experiments where DSDV showed better agility than DYMO.

Observation 17 *Although DYMO showed inferior agility in previous experiments, the continuously changing topology depicted in experiment (10) is handled well by DYMO when other protocols faced problems in ensuring a continuous connectivity and thereby throughput especially on the IEEE 802.11g MAC.*

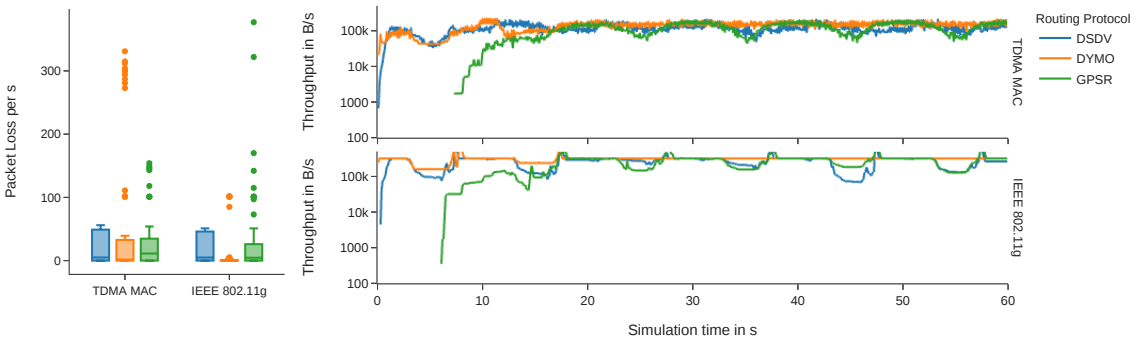

a) Number of packets lost per second

b) Application data throughput on receiving node

Figure 4.23: Measurements recorded at the experiment *(11)* of the *generated experiments* group

The second experiment of the *alternative route experiments* group implements an extension of experiment *(04)* where instead of a direct connection from the sender to the receiver, a route with a single hop is always necessary. All of the utilized routing protocols are capable of delivering a continuous throughput, see Figure 4.23b where DYMO is even capable of delivering a stable throughput later in the simulation. DSDV and GPSR are experiencing a regular drop in throughput created by the emerging node Ⓒ. This is confirmed by the observed packet loss in Figure 4.23a where DYMO features the lowest packet loss of all the routing protocols regardless of the utilized MAC.

Figure 4.24a visualizes the number of hops a successfully transmitted packet on the destination node visited including the destination node itself. All routing protocols are mainly using the route over node Ⓓ whereas DSDV and GPSR routed in a loop in individual simulation runs. The observation of the amount of processed packets on the network's nodes reveals that DYMO is successfully avoiding routes over Ⓒ, whereas DSDV is utilizing Ⓒ

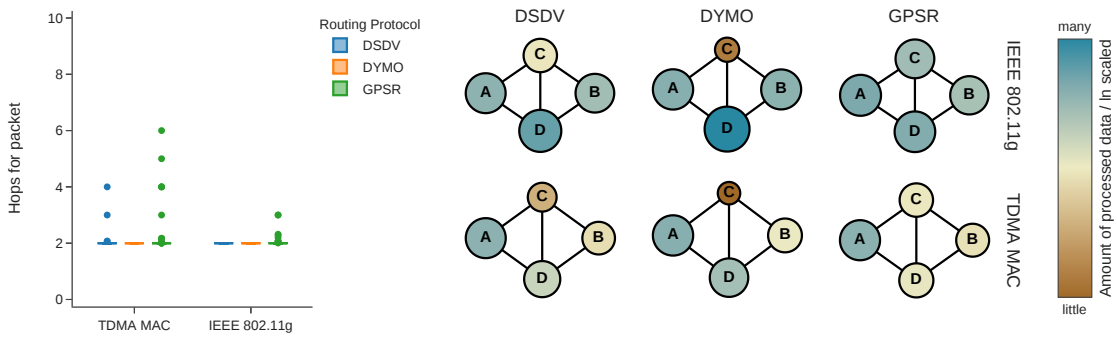

a) Visited hops for received packets

b) Processed data volume for each node

Figure 4.24: Measurements recorded at the experiment *(11)* of the *generated experiments* group visualizing route selection

for a minority of packets and GPSR is regularly using Ⓒ. However, all routing protocols are still preferring routes over Ⓓ although in the case of GPSR the preference is weak when compared to DSDV or DYMO.

Observation 18 *All routing protocols are capable of utilizing an alternative stable route, whereas DYMO performed good in this experiment but DSDV and GPSR were not fully avoiding the unstable route.*

4.1.4 Energy Consumption

The simulation environment implemented in this work is not capable of realistically simulating the actual energy consumption of the network's nodes as the TDMA MAC is implemented to mimic the behavior of DLR's MAC but not implementing a physically accurate model. However, it is possible to estimate the energy consumption by comparing the utilization of the MAC at each node within the network. The already analyzed protocol overhead introduced by a routing protocol leads to more data being transmitted on the MACs of the nodes. A lower protocol overhead results in less energy consumption of the nodes. As most of the experiments conducted in this work force the utilization or avoidance of specific nodes within the network, the analysis of the energy consumption will focus on experiment *(07)* which features a defined layout and enough nodes for a routing protocol to choose alternative routes.

In Figure 4.25 the observed routing protocol overhead is visualized for each of the utilized MACs. The overhead observed for all the routing protocols is very similar, whereas DSDV is featuring regular peaks due to the proactive nature of the protocol. The overhead of all routing protocols is larger in the beginning of the simulation and lowers after the initial setup of the routes. This is created by no application packets being transmitted at the beginning of the simulation. While DYMO also features peaks at the beginning of simulations implementing outward movement, this is not the case for inward movement as DYMO is not changing the established route after inward movement. The overhead created by GPSR is very low after initial beaconing as the positioning information of the nodes is attached to

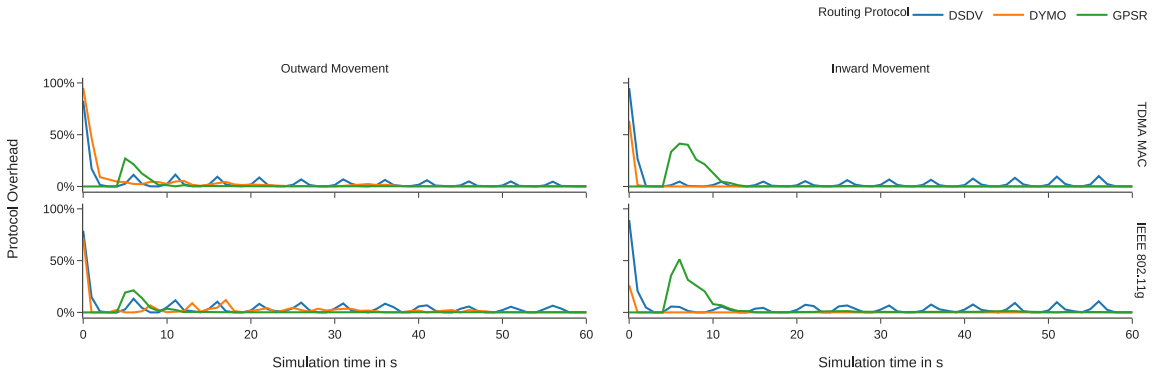

Figure 4.25: Measured routing protocol overhead relative to all transmitted application packets regarding the movement direction over time in experiment *(07)*

the transmitted application packets. Therefore no additional routing protocol packets are recorded by the metric.

Observation 19 *DYMO and GPSR achieve a low overhead once initial routes are setup. However, GPSR is attaching its overhead to the application packets which still increases the utilization of the MAC and therefore still consuming additional energy. Due to the proactive operation of DSDV, the overhead stays the same throughout the whole simulation.*

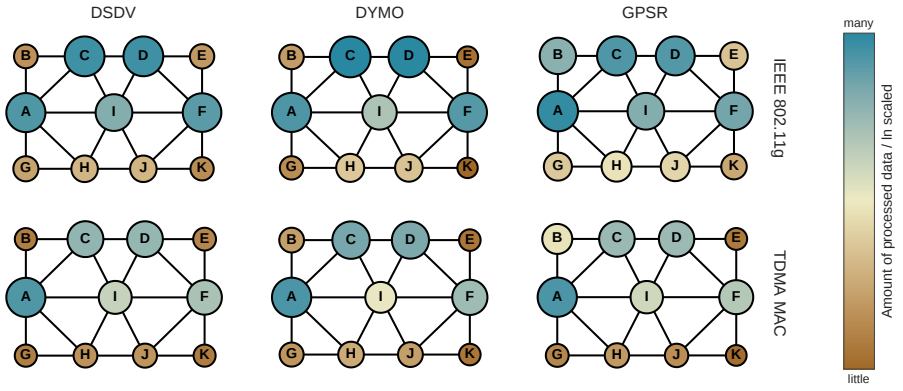

Figure 4.26: Comparison of the amount of processed incoming and outgoing data for each node in experiment *(07)*

Additionally to the overhead created by the routing protocol, the routing decisions have a direct impact on the utilization of neighboring nodes. By aggregating the amount of sent and received data for each node and averaging it over all simulation runs, the utilization of the nodes can be visualized and thereby compared. Figure 4.26 shows the amount of processed data on each node in the network for the experiment *(07)* of the *advanced experiments* group. Due to the separation of the network described in Section 3.2.3 the lower half of the network is naturally less utilized. Nevertheless, all routing protocols were

capable of utilizing the lower half of the network, although far less utilization than seen in the upper half of the network. As already seen in previous observations, the DYMO routing protocol will not change an established route unless it gets unavailable. Therefore, the load distribution of the nodes is concentrated on the stable path from source to destination over Ⓒ and Ⓓ. The shorter path over Ⓘ is only used outward movement of the lower half of the network. DSDV is showing a more balanced utilization between the two paths, although featuring very low utilization of all the other nodes. The greedy operation of GPSR leads to a higher utilization of the other nodes which are not on one of the two main routes. This is in accordance with the observation of longer routes established by GPSR in the simulations.

Observation 20 *Generally, the load distribution of processed data within the network is heterogeneous despite minor differences in the utilization of each of the routing protocols.*

CHAPTER 5

Conclusion

This chapter will summarize the contribution of this work in implementing a network simulation environment suitable to assess the differences of routing protocol operation embedded in in-situ space exploration missions utilizing the MAC of DLR. The experiment designs proposed in this work along with the observations made during the execution of simulations implementing these designs will be summarized and conclusions will be drawn.

5.1 Summary

This work implements a simulation design for the evaluation of routing protocols in the context of ad-hoc wireless networks. Within these networks a wireless MAC by DLR purpose-built for in-situ space exploration missions is utilized on the network's nodes. This MAC is primarily focused on missions to Moon and Mars and is very similar to a standard IEEE 802.11g MAC with the main difference being the utilization of a TDMA based channel access. This channel access scheme has influence on the behavior of the MAC observable by upper layers in the network stack. The simulation environment built in this work is based on the *Omnet++* framework with the `INET` framework libraries. The TDMA channel access has been implemented for the `INET` framework and integrated into the existing IEEE 802.11g MAC and resembles the DLR MAC within the simulation. Additionally to the DLR MAC, the simulation implements an environment which features real terrain data of the Moon collected by the LRO mission. This allows the implementation of experiment designs which utilize the unique terrain shape found on the Moon. The design of these experiments was divided in 5 categories: the *simple experiments* group, the *basic agility experiments* group the *advanced experiments* group, the *generated experiments* group, and the *alternative route experiments* group. Each of the experiment groups feature experiment designs of varying complexity and examine different aspects of a routing protocol's behavior. Starting with the *simple experiments* group the most basic operation of the routing protocols is tested. This includes revealing potential delays in route establishment, the impact on application data throughput, additional packet losses, and the overhead introduced by a routing protocol due to additional packets being transmitted in the network. Continuing with the *basic agility experiments* group, the networks are advanced with one additional node appearing or leaving the network mid-simulation. The additional node is not always

necessary for a successful communication between the source and destination node. The group primarily tests the reaction of routing protocols to minimal changes in topology which may not always be relevant to the route between source and destination node. The *advanced experiments* group implements more complex experiments which implement multiple active routes within a single network and a network fragmentation due to a separation of nodes caused by movement. The fourth experiment group focuses on varying the amount of nodes featured in an experiment. This is achieved by generating experiment layouts where nodes are placed in the network by a given layout. The last experiment group depicts experiments with highly dynamic topologies. The shortest route within these networks is not always a stable route where alternative and possibly longer routes yield better connection stability.

The experiments were simulated with a number of different parameters and the evaluation of the results yielded a variety of different observations. From these observations it can be concluded that applications and routing protocols running on the TDMA MAC are generally performing more unstable than on the IEEE 802.11g MAC, see Observation 1 and 2. Utilizing specialized applications and routing protocols which are aware of the TDMA scheme of the MAC will avoid these instabilities. Furthermore, the Observation 3 showed that the built-in order in which nodes are processing packet reception and transmission creates a bias in the route establishment of the protocols where the node first in line of the TDMA slot indices achieved higher application data throughput. Apart from the differences in operation found on the MACs, the individual routing protocols showed differences in the time needed to adopt to new topologies. The proactive DSDV and greedy GPSR protocols in general showed better performance in reacting to topology changes than DYMO, see Observation 6 and 7. As DYMO has only been tested in the default configuration provided by the `INET` framework, the reaction time of the routing protocol can be improved by choosing different timing configurations. However, this timing configuration should be decided upon individually for each in-situ space exploration mission to match the specific requirements of that mission. The performance of the GPSR protocol was surprisingly unstable, especially with regards to finding short and stable routes as repeatedly seen Observations 9, 10, 11, 12, and 16. As this work introduced minor patches regarding distance and angle calculations to the GPSR implementation of `INET` to make the GPSR implementation compatible with the simulation environment of this work as described in Section 3.1.1, a faulty or incompatible implementation of the protocol in the `INET` framework can not be completely eliminated. However, in the past several shortcomings in the GPSR protocol have been identified revealing similar observations [41]. This creates confidence into the soundness of the results gained on the GPSR protocol. While DSDV was always capable of finding the shortest route to the destination, DYMO preferred already established routes and only changed a route when it became unavailable, see Observation 13. In situations with highly dynamic topology DYMO featured the best performance and provided the most stable and highest throughput, see Observations 17 and 18. However, this result can be biased by the patches introduced to the GPSR protocol to ensure operation within the simulation environment and the DSDV routing protocol implementation within `INET` being incomplete as indicated in the `INET` documentation [42]. The observation of the amount of processed data on the nodes within the network revealed a heterogeneous distribution of load for all routing protocols, as seen in Observations 19 and 20. This causes an unequal consumption of energy for the nodes within the network and may lead to an early failure of highly utilized nodes. This effect can be counteracted by utilizing a routing protocol adhering the consumption of

energy on the nodes and incorporating the energy level of the nodes into routing decisions. Alternatively, the nodes with low energy consumption can exchange positions with highly utilized nodes and thereby balancing the overall energy consumption in the network over time.

5.2 Future Work

The featured experiment designs in this work are not limited to the application in in-situ space exploration but are also valid choices for ad-hoc networks in use here on earth. The experiment designs are capable of hosting other environments such as urban environments, forests, or other natural landscapes such as the arctic or deserts. Furthermore, the simulation can be extended to host more ad-hoc routing protocols. The utilization of different routing protocols implementing similar routing strategies (proactive, reactive, and greedy geographic) could reveal insight into the impact of the routing strategy on the performance of the protocols. Additionally, the implementation of the routing protocols utilized in this work taken from the `INET` framework can be evaluated for implementation errors and the aforementioned missing parts of the DSDV protocol added to the `INET` framework to better assess the results of this work. Further, the routing protocols can be adjusted to incorporate the TDMA scheme of DLR's MAC to overcome the unstable operation of the protocols. Especially the GPSR protocol can benefit from specialization on DLR's MAC as the MAC automatically gains knowledge on neighboring nodes without transmitting any packets after a single TDMA cycle due to the builtin localization system of that MAC [11]. The experiments in this work are simulated for a duration of up to 80 s. By adjusting the design of the experiments in this work, the experiments can be extended to be simulated for a much longer duration which might yield further insight into the long-term operation of the routing protocols within the depicted scenarios. Ultimately, the results of this work can be verified by implementing the experiments of this work in a real world application outside a simulation environment. As some of the experiment designs require complex setups, the verification of the experiment results outside a simulation environment may start with the simple experiment designs of the first two experiment groups.

Bibliography

[1] ISECG. *The Global Exploration Roadmap*. Aug. 2020.

[2] Claire R. Cousins and Charles S. Cockell. "An ESA roadmap for geobiology in space exploration". In: *Acta Astronautica* 118 (Jan. 2016), pp. 286–295.

[3] Yang Gao and Steve Chien. "Review on space robotics: Toward top-level science through space exploration". In: *Science Robotics* 2.7 (2017).

[4] G. A. Landis and P. P. Jenkins. "Dust on Mars: Materials Adherence Experiment results from Mars Pathfinder". In: *Conference Record of the Twenty Sixth IEEE Photovoltaic Specialists Conference - 1997*. IEEE, 1997, pp. 865–869.

[5] A. H. Mishkin et al. "Experiences with operations and autonomy of the Mars Pathfinder Microrover". In: *1998 IEEE Aerospace Conference Proceedings (Cat. No.98TH8339)*. Vol. 2. IEEE, 1998, 337–351 vol.2.

[6] S. W. Squyres et al. "Two Years at Meridiani Planum: Results from the Opportunity Rover". In: *Science* 313.5792 (2006), pp. 1403–1407.

[7] R. Sternberg et al. "Gas chromatography in space exploration: Capillary and micropacked columns for in situ analysis of Titan's atmosphere". In: *Journal of Chromatography A* 846.1-2 (June 1999), pp. 307–315.

[8] Paul R. Mahaffy et al. "Abundance and Isotopic Composition of Gases in the Martian Atmosphere from the Curiosity Rover". In: *Science* 341.6143 (2013), pp. 263–266.

[9] Mariah M. Baker et al. "The Bagnold Dunes in Southern Summer: Active Sediment Transport on Mars Observed by the Curiosity Rover". In: *Geophysical Research Letters* 45.17 (Sept. 2018), pp. 8853–8863.

[10] Emanuel Staudinger et al. "Swarm Technologies For Future Space Exploration Missions". In: June 2018.

[11] Siwei Zhang et al. "Assembling a Swarm Navigation System: Communication, Localization, Sensing and Control". In: *1st International Workshop on Communication and Networking for Swarms Robotics*. 2021.

[12] X. Hong et al. "The Mars sensor network: efficient, energy aware communications". In: *2001 MILCOM Proceedings Communications for Network-Centric Operations: Creating the Information Force (Cat. No.01CH37277)*. Vol. 1. 2001, 418–422 vol.1.

[13] David B. Johnson and David A. Maltz. “Dynamic Source Routing in Ad Hoc Wireless Networks”. In: *Mobile Computing*. Ed. by Tomasz Imielinski and Henry F. Korth. Vol. 353. The Kluwer International Series in Engineering and Computer Science. Kluwer / Springer, Jan. 1996, pp. 153–181.

[14] C. E. Perkins and E. M. Royer. “Ad-hoc on-demand distance vector routing”. In: *Proceedings WMCSA'99. Second IEEE Workshop on Mobile Computing Systems and Applications*. IEEE, 1999, pp. 90–100.

[15] Oskar Wibling, Joachim Parrow, and Arnold Pears. “Automatized verification of ad hoc routing protocols”. English. In: *Formal techniques for networked and distributed systems – FORTE 2004. 24th IFIP WG 6.1 international conference, Madrid, Spain, September 27–30, 2004. Proceedings*. Berlin: Springer, Sept. 2004, pp. 343–358.

[16] R. Ramanathan and J. Redi. “A brief overview of ad hoc networks: challenges and directions”. In: *IEEE Communications Magazine* 40.5 (5 May 2002), pp. 20–22.

[17] Dimitar Trajanov and Sonja Filiposka. “Small world application layer for ad hoc networks”. In: *Conference: Telekomunikacioni Forum Telfor*. Jan. 2003.

[18] Charles E. Perkins and Pravin Bhagwat. “Highly Dynamic Destination-Sequenced Distance-Vector Routing (DSDV) for Mobile Computers”. In: *SIGCOMM Comput. Commun. Rev.* 24.4 (Oct. 1994), pp. 234–244.

[19] D. Johnson, Y. Hu, and D. Maltz. *The Dynamic Source Routing Protocol (DSR) for Mobile Ad Hoc Networks for IPv4*. RFC 4728. RFC Editor, Feb. 2007.

[20] Chalermek Intanagonwiwat, Ramesh Govindan, and Deborah Estrin. “Directed diffusion: a scalable and robust communication paradigm for sensor networks”. In: *MOBICOM 2000, Proceedings of the sixth annual international conference on Mobile computing and networking, Boston, MA, USA, August 6-11, 2000*. Ed. by Raymond L. Pickholtz et al. ACM, 2000, pp. 56–67.

[21] Xiaoyan Hong et al. “Load balanced, energy-aware communications for Mars sensor networks”. In: *Proceedings, IEEE Aerospace Conference*. Vol. 3. 2002, pp. 3–3.

[22] C. Perkins, E. Belding-Royer, and S. Das. *Ad hoc On-Demand Distance Vector (AODV) Routing*. RFC 3561. RFC Editor, July 2003.

[23] Dong-Won Kum et al. “Performance Evaluation of AODV and DYMO Routing Protocols in MANET”. In: *2010 7th IEEE Consumer Communications and Networking Conference*. IEEE, Jan. 2010, pp. 1–2.

[24] Brad Karp and H. T. Kung. “GPSR: Greedy Perimeter Stateless Routing for Wireless Networks”. In: *Proceedings of the 6th Annual International Conference on Mobile Computing and Networking*. MobiCom '00. Boston, Massachusetts, USA: Association for Computing Machinery, 2000, pp. 243–254.

[25] Chaoyue Xiong, Tadao Murata, and Jeffery Tsai. “Modeling and Simulation of Routing Protocol for Mobile Ad Hoc Networks Using Colored Petri Nets”. In: *Proceedings of the Conference on Application and Theory of Petri Nets: Formal Methods in Software Engineering and Defence Systems - Volume 12*. CRPIT '02. Adelaide, Australia: Australian Computer Society, Inc., 2002, pp. 145–153.

[26] Kristian L. Espensen, Mads K. Kjeldsen, and Lars M. Kristensen. “Modelling and Initial Validation of the DYMO Routing Protocol for Mobile Ad-Hoc Networks”. In: *Applications and Theory of Petri Nets*. Ed. by Kees M. van Hee and Rüdiger Valk. Berlin, Heidelberg: Springer Berlin Heidelberg, 2008, pp. 152–170.

[27] F. de Renesse and A. H. Aghvami. “Formal verification of ad-hoc routing protocols using SPIN model checker”. In: *Proceedings of the 12th IEEE Mediterranean Electrotechnical Conference (IEEE Cat. No.04CH37521)*. IEEE, 2004.

[28] Tommaso Ghidini. “Materials for space exploration and settlement”. In: *Nature Materials* 17.10 (Sept. 2018), pp. 846–850.

[29] Terrence Fong and Illah Nourbakhsh. “Interaction Challenges in Human-Robot Space Exploration”. In: *Interactions* 12.2 (Mar. 2005), pp. 42–45.

[30] Antonio Ceballos et al. “A Goal-Oriented Autonomous Controller for space exploration”. In: *Proceedings of the ASTRA 2011, 11th Symposium on Advanced Space Technologies in Robotics and Automation* (Jan. 2011).

[31] Kurt Sacksteder and Gerald Sanders. “In-Situ Resource Utilization for Lunar and Mars Exploration”. In: *45th AIAA Aerospace Sciences Meeting and Exhibit*. American Institute of Aeronautics and Astronautics, Jan. 2007.

[32] Gerald B. Sanders. “Advancing In Situ Resource Utilization Capabilities To Achieve a New Paradigm in Space Exploration”. In: *2018 AIAA SPACE and Astronautics Forum and Exposition*. American Institute of Aeronautics and Astronautics, Sept. 2018.

[33] JIA Yingzhuo XU Lin ZOU Yongliao. “China’s Planning for Deep Space Exploration and Lunar Exploration before 2030”. In: *Chinese Journal of Space Science* 38.5, 591 (2018), p. 591.

[34] Hao Chen et al. “Integrated in-situ resource utilization system design and logistics for Mars exploration”. In: *Acta Astronautica* 170 (May 2020), pp. 80–92.

[35] Andras Varga. “OMNeT++”. In: *Modeling and Tools for Network Simulation*. Ed. by Klaus Wehrle, Mesut Güneş, and James Gross. Berlin, Heidelberg: Springer Berlin Heidelberg, 2010, pp. 35–59.

[36] M.A. Ivanov et al. “Landing site selection for Luna-Glob mission in crater Boguslawsky”. In: *Planetary and Space Science* 117 (Nov. 2015), pp. 45–63.

[37] Maria T. Zuber et al. “The Lunar Reconnaissance Orbiter Laser Ranging Investigation”. In: *Space Science Reviews* 150.1-4 (May 2009), pp. 63–80.

[38] INET Developers. *The Transmission Medium*. Accessed: 2021-04-03. URL: `https://inet.omnetpp.org/docs/users-guide/ch-transmission-medium.html`.

[39] William Jakes. *Microwave Mobile Communications*. New York: John Wiley & Sons, May 2, 1994. 660 pp.

[40] INET Developers. *Wireless Signal Analog Domain Representations*. Accessed: 2021-01-21. URL: `https://inet.omnetpp.org/docs/showcases/wireless/analogmodel/doc/index.html`.

[41] Andrey Silva, Niaz Reza, and Aurenice Oliveira. “Improvement and Performance Evaluation of GPSR-Based Routing Techniques for Vehicular Ad Hoc Networks”. In: *IEEE Access* 7 (2019), pp. 21722–21733.

[42] INET Developers. *API Reference for the DSDV Module in INET*. Accessed: 2021-04-02. URL: https://doc.omnetpp.org/inet/api-current/neddoc/inet.routing.dsdv.Dsdv.html.

Appendix

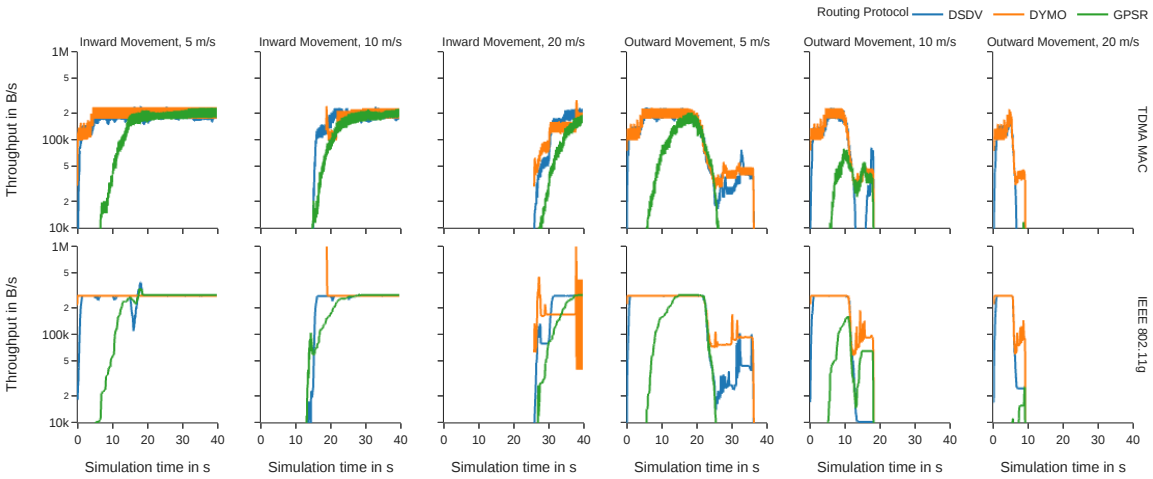

Figure A.1: Application data throughput on receiving node regarding speed and movement direction over time in experiment *(05)* comparing the utilized MACs and routing protocols

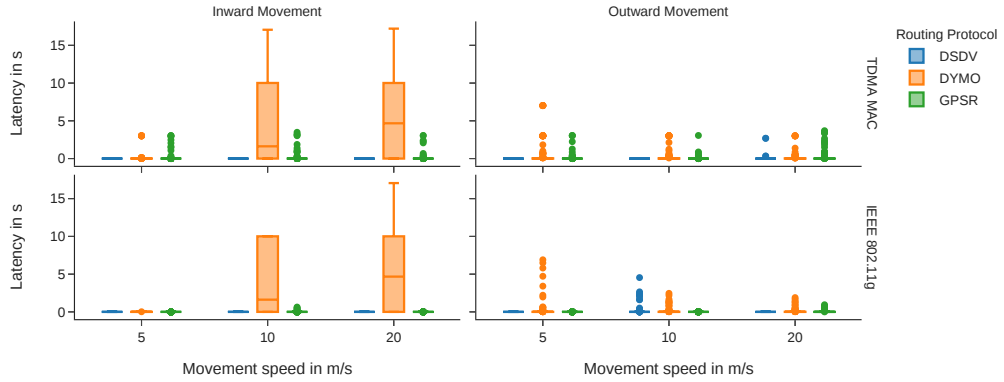

Figure A.2: Measured route establishment latency for each routing protocol on both utilized MACs in experiment *(05)*

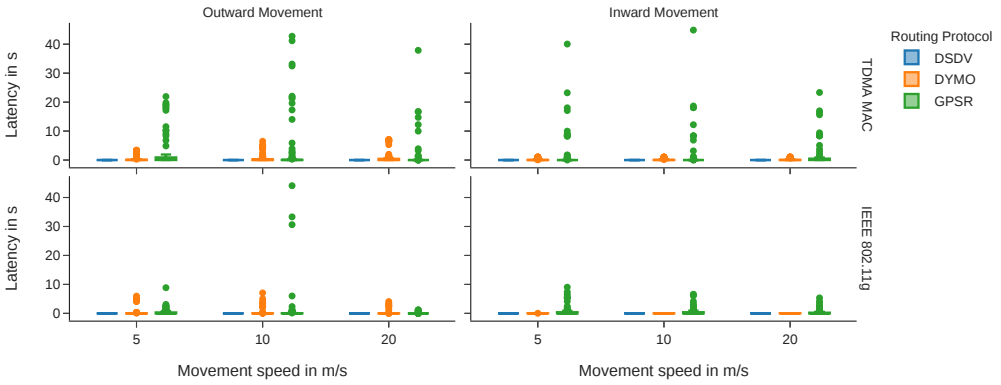

Figure A.3: Measured route establishment latency for each routing protocol on both utilized MACs in experiment *(07)*